Authors' response to Referee #1:

We would like to thank the referee for reviewing this manuscript, the valuable feedback and the very constructive comments. At this stage of the review process, we respond to the referee #1's comments and propose improvements for the final manuscript. The referee's original comments are printed in **bold** followed by the corresponding answers. Passages from the manuscript are printed in *italic writing*, in which proposed additions are indicated in blue and deleted parts in ~~red~~.
Thank you very much for your efforts,

Jan Bartl on behalf of all authors

Overall comment (1a)

Symmetry: Sometimes I became a little confused about discussions on symmetry. At some points (page 12 for example) the focus was on the shape of curl, but on bottom page 14, I had the impression symmetry here meant a difference in the effectiveness of positive versus negative yaw. Maybe this could be further clarified.

Thank you for this very constructive comment. Indeed, the term 'symmetry' refers to two different parameters in those cases, which should be further clarified. On the top of page 12 the symmetry of the shape of wake curl is analyzed, while further down (bottom of page 12 to bottom of page 14) the symmetry in effective wake deflection is compared. In both cases, however, the symmetry is analyzed with respect to positive versus negative yaw angles. In the comparison on page 12, the three-dimensional wake scans behind a positively and negatively yawed turbine are parametrized to two-dimensional curves showing local velocity minima. In the comparison on page 14, however, the three-dimensional wake scans are parametrized to a single value quantifying the overall wake deflection. For clarification, the following changes are suggested for the manuscript:

p.12, l.1 ff:
Wake curl symmetry
In order to compare the three-dimensional wake shapes behind a positively versus negatively yawed turbine more quantitatively, the curled shapes of the velocity deficit area are parametrized to a two-dimensional line. For this purpose, the minimum values in streamwise velocity $\overline{u}/u_{ref}$ are extracted from the fitted wake contours for each vertical position ranging from y/D=[-0.5, ..., 0.5]. The detailed method is described in Section 3.1.

p.12, l.20 ff:
Overall wake ~~center~~ deflection
The ~~3D~~ three-dimensional Available power method ~~introduced in Section 3.2~~ is used to quantify the overall deflection of the kinetic energy contained in the wake. As

explained in Section 3.2 the minimum available power in a circular area in the wake is located, which is reducing the full wake flow field to a single parameter representing the overall wake deflection. A comparison of the minimum available power in the wakes behind a positively versus negatively yawed turbine enables a comparison of symmetry in the deflection of the energy contained in the wake with respect to the yaw angle. Additionally, a ~~2D~~ two-dimensional Gaussian fit method ~~are used for the quantification of wake deflection.~~ for the wake center detection at the turbine's hub-height is used to demonstrate systematic differences in the deflection quantification methods

p.14, l.5 f:
A systematic asymmetry in the wake deflection represented by the minimum available power behind a turbine yawed $\gamma = -30°$ and $\gamma = +30°$ is observed.

Overall comment (1b)

Further, if I understand, both asymmetries are explained as being explained by interaction with the tower. This made sense to me in the discussion of the symmetry of the wake itself, but I had some doubts if it could fully explain the asymmetry in +/- effectiveness. For example, some LES codes show this asymmetry while not including any tower model in the flow (for example ALM, or ADM codes which have essentially only the rotor modeled). Wouldn't this imply some other mechanisms could also be responsible?

Thank you for this very good comment. This is one of the very substantial questions that require to be clarified when discussing possible causes for deflection asymmetries during wake steering. Yes, we deem the interaction of the rotor wake and tower wake to be the main reason for the slight asymmetries in both the wake curl and also the resulting overall wake deflection. The tower structure and its wake introduce an asymmetry to the otherwise perfectly symmetrical setup. However, other mechanisms can potentially affect the wake deflection symmetry, especially in the case of full-scale turbines. These are discussed in the following:

Mechanisms that generally can introduce asymmetry to a yawed turbine setup:
(1) non-uniform inflow to the rotor, e.g. shear or veer
(2) ground effects/wall blockage effects
(3) systematic errors in turbine yaw alignment
(4) tower wake interaction

(1) The effects of a vertical sheared inflow on wake steering through yaw was recently investigated in an experiment by Schottler et al. (2017a). They found an asymmetric power distribution of an aligned downstream turbine with respect to the upstream turbine yaw angle, when a strong vertically sheared profile was present in the inflow. By inverting the vertical shear in the inflow, the power distribution of the downstream turbine was again asymmetric, however towards the opposite sign of the upstream

turbine yaw angle.
Asymmetries in the deflection of the yawed wake are simulated in a LES by Vollmer et al. (2016), in which a combination of inflow shear and veer are deemed to be responsible for the asymmetric wake shapes especially in stable atmospheric conditions. An asymmetric combined power distribution is also observed in another LES study on full-scale turbines by Fleming et al. (2015), where the turbines are exposed to a LES-generated atmospheric boundary layer. Therein, Coriolis forces and wind veer are discussed as a reason for differences in wake deflection. In a recent follow-up study by Fleming et al. (2017) veer is kept to a minimum and no deflection of the non-yawed baseline case is observed. The deflection asymmetries of the yawed wake are explained with a difference in vortex interaction with the shear in the neutral atmospheric boundary layer.
In the test cases A and B of this study, however, neither shear or veer are present in the inflow. Nevertheless, a slight asymmetry in overall wake deflection is present, implying that other mechanisms might be the main reasons in these cases.

(2) Secondly, possible ground or side wall blockage effects are discussed. The experimental setup is perfectly symmetrical, i.e. the rotor is located in the center of the wind tunnel meaning that it has the same distance to wind tunnel floor and roof respectively the right and left sidewall. The boundary layer on floor, roof and both sidewalls is measured to be $d_{BL,3D} \approx 20cm$ respectively $d_{BL,6D} \approx 25cm$. The rotor swept area blocks 12.8% of the wind tunnel cross sectional area, which affects the wake development. A LES study by Sarlak et al. (2016) showed, however, that the wake expansion is only insignificantly affected by blockage ratios smaller than 20%. For a deflected wake behind a yawed turbine, however, interactions with the sidewalls cannot be excluded anymore, especially for the higher downstream distance $x/D = 6$. Although the distance to each sidewall is equal, it is possible that the wake deflection is blocked to a higher degree by right sidewall (for $\gamma = +30°$) than by the left sidewall (for $\gamma = -30°$). This scenario is considered to be unlikely, however, only a high-fidelity simulation with and without wind tunnel walls could clarify this completely.

(3) As a third source for wake deflection asymmetries, systematic errors in the turbine yaw alignment should be discussed. The correct alignment at $\gamma = 0°$ is ensured by installing horizontal laser sheets at the central points of the wind tunnel and adjusting the turbine yaw angle to it. The yaw angle itself is adjusted with a calibrated fully automatic turntable. Inaccuracies in the experimental setup can never be excluded, however, the accuracy of the yaw angle adjustment was estimated to be within $\pm 1°$. Experiments with the model turbine by ForWind as reported in the companion paper by Schottler et al. (2018) show a very symmetric wake deflection with respect to positive and negative yaw angles in an otherwise identical setup. This indicates that the slight differences in wake deflection have to be dependent on the turbine geometry or wall blockage.

(4) The final possible source for asymmetries to be discussed is the rotor wake's interaction with the tower wake. On the same rotor as used in this study, Pierella and Sætran (2017) showed that the presence of the tower wake induced significant non-symmetries in the rotor wake caused by *"a different cross-stream momentum transport in the top-*

tip and bottom-tip region." For a non-yawed turbine operated at its optimum tip speed ratio, they showed that the center of the wake vortex is slightly deflected downwards and to the left with increasing downstream distance. They are able to clearly attribute this effect to the interaction with the tower wake. As counter-evidence they managed the wake to recover its symmetric structure by installing a second mirrored turbine tower from the nacelle to the wind tunnel roof.
Pierella and Sætran's experiment indicates both a lateral and vertical displacement of the wake vortex center through the interaction with the tower wake. For the yawed case, the interaction of the counter-rotating vortex pair with the slightly displaced wake vortex might lead to a slightly differently displaced wake behind a positively and negatively yawed turbine. At this stage we only can guess about the exact interaction mechanisms, but a tower-wake-induced displaced wake vortex in the non-yawed case supports the assumption of an asymmetrically displaced wake center for the yawed cases.
In comparison to Pierella and Sætran's tower wake experiment, a slimmer tower was constructed for the new yaw experiments ($D_{tower,old} = 61mm$ vs $D_{tower,new} = 43mm$) in order to minimize tower wake effects and adjust the geometrical scaling to a full-scale setup. The geometrical scaling of the tower now fits very well with that of a full-scale turbine (e.g. NREL 5MW reference turbine, Jonkman et al., 2009):

$$\frac{D_{tower,exp}}{D_{rotor,exp}} = \frac{0.043m}{0.894m} \approx \frac{D_{tower,NREL-5MW-ref}}{D_{rotor,NREL-5MW-ref}} = \frac{6m}{126m}$$

However, a significantly larger tower drag coefficient is expected in the small-scale experiment than for a full-scale turbine. Assuming a tower diameter of

$$D_{tower,NREL-5MW-ref} = 6m$$

for a full-scale turbine, we can calculate a Reynolds number of

$$Re_{D,tower,NREL-5MW-ref} \approx 4 \times 10^6.$$

According to Schlichting (1968), this is in the transition region resulting in a drag coefficient of about

$$C_{D,tower,NREL-5MW-ref} \approx 0.3.$$

In our model scale experiment, however, the tower-based Reynolds number is as low as

$$Re_{D,tower,exp} \approx 3 \times 10^4,$$

resulting in a much higher drag coefficient of

$$C_{D,tower,exp} \approx 1.0.$$

Consequently, the effect of the tower wake on the rotor wake (and thus also deflected rotor wakes) is deemed to be significantly stronger in the Re-range of model-scale experiments than in full-scale situations

We share the opinion that this line of arguments for a significant influence of the tower wake on the wake deflection is not sufficiently explained in the manuscript yet. As this is a very critical issue, we suggest to add some more lines to the explanation on p.14:

p.14, l.5 ff:
The wake shows a higher deflection for negative yaw angles in all inflow cases. Also the wake behind the non-yawed turbine is seen to be slightly deflected in positive z-direction, which is assumed to stem from the interaction of the rotating wake with the turbine tower. As discussed by Pierella and Sætran (2017) who performed experiments on the same rotor with a slightly larger tower, the tower-wake interaction ~~can lead~~ leads to an uneven momentum entrainment in the wake. For the non-yawed case Pierella and Sætran (2017) observed both a lateral and vertical displacement of the wake vortex center, induced by an interaction with the tower wake. It can therefore be assumed that also the interaction of the counter-rotating vortex pair with the tower wake slightly displaced wake vortex in the yawed cases might be influence by an interaction with the tower wake, which is the only source of asymmetry in an otherwise perfectly symmetrical setup.

Overall comment (1c)

A final point on this discussion, could you include some discussion of the proximity of the rotor to the ceiling and the floor? I was thinking a source of discrepancy might be that LES/field data will have only a ground, and as a result only one of the vortices experiences ground effects. Is this a consideration?

This is indeed a very good thought. When discussing ground effects two different phenomena can be referred to:
(1) the presence of the ground in an otherwise uniform flow
(2) the formation of a boundary layer shear through ground friction

(1) The influence of ground effects on the interaction of a counter-rotating vortex pair (CVP) in the wake for an Actuator disc exposed to a uniform inflow has been discussed in a computational free-wake vortex filament study by Berdowski et al. (2018). In this study, ground effects could be isolated by running two different simulations, of which only one was including a symmetry plane on the ground. For this case they observed that *the bottom vortex of the CVP forms another CVP with its mirror vortex underground and in opposite direction.* (Berdowski et al., 2018)
As shown in Fig. 6 (c) in the manuscript, we did not observe this effect in our perfectly symmetrical experimental setup, in which both the ground and also the roof of a wind tunnel are present. Our model turbine ($D \approx 90cm$) is installed with a hub height ($h_{hub,exp} = 89cm$) adjusted to the center of the wind tunnel ($h_{tunnel} \approx 180cm$). That means that about half a rotor diameter ($45cm$) of space is left for the freestream flow

above and below the rotor. The proximity of the rotor to the floor roughly scales with that of a full-scale turbine ($h_{hub,NREL-5MW-ref} = 90m$). However, the same proximity to the ceiling is unrealistic, but was chosen to specifically to ensure the best possible symmetry in the setup and to avoid interactions with the wind tunnel boundary layers ($d_{BL} \approx 20 - 25cm$). Outside of these boundary layers the inflow is spatially uniform within ±0.8% (Inflow A) and ±2.5% (Inflow B).

(2) In contrast to most field data and also the referenced LES simulations, where a certain amount of shear (and sometimes also veer) is present, the inflow in the wind tunnel experiment is completely uniform (Inflows A and B). That means that apart from the previously discussed tower wake effects, the interaction of the different wake vortices should be "clean" and not biased by shear or veer in the inflow. However, one could argue that the two vortices of the counter-rotating vortex pair could expand differently in a full-scale situation as the expansion of the lower vortex is limited by the ground while the upper one can expand freely. The blocked expansion of the wake and its single structures is definitely an issue in wind tunnel experiments, which becomes more serious for increasing downstream distances. It cannot be excluded that the dimension and strength of the single vortices is also influenced by wall effects in this experiment. However, comparisons of the general wake structures with experiments behind smaller, unblocked rotors show a good agreement as shown in Schottler et al. (2018) and Bartl et al. (2018). In general, it must be kept in mind that the results of this wind tunnel campaign do not reflect realistic conditions at all. A number of discrepancies as the simplifications in the inflow and especially the wall blockage can be considered as strong disadvantages to full-scale measurements and simulations. However, the controlled boundary conditions of a wind tunnel experiment allow to isolate the influence of certain parameters, i.e. inflow shear and turbulence, in a controlled manner. This can be an advantage over full-scale measurement and additionally serve as well-defined reference data for the validation of CFD codes.

Overall comment (2)

A second overall comment, the authors point out that is difficult to reduce wake deflection to a single value, and can complicate interpretation of results such as Fig 8-9. Since you already employ the method of available power, I believe an interesting additional comparison between the collected data and the models would be to compare the power output of an imaginary turbine located at x/D=6 and z/D=0 (and perhaps z/D = +/- 0.5). This could represent an interesting assessment of do the models correctly predict the change in power obtained through wake steering for a given arrangement.

Thank you for this very good comment. This is indeed a very good idea as we actually have performed measurements available with an offset downstream turbine operated at $x/D = 3$. Seven different lateral offsets of the downstream turbine z/D have been chosen ranging from $z/D = [-0.50, -0.33, -0.16, 0, +0.16, +0.33, +0.50]$. Power measurement have been performed for the upstream turbine yaw angles $\gamma_{T1} = 0°$ and $\gamma_{T1} = 30°$. A comparison of the *Available Power* calculated from mean streamwise velocity distribution in the wake with the actually measured power coefficient $C_{P,T2}$ of

a downstream rotor traversed through the wake is presented in Fig. 1.
The comparison generally shows a good match between the measured downstream turbine power and the calculated *Available Power* in the wake flow for both upstream turbine yaw angles. These results show that the *Available Power Method* generally performs as it should for the purpose of reducing the wake deflection to a single value. However, the coarse grid of only seven z/D-positions does not enable us to validated the exact location of the calculated minimum *Available Power*. For the calculation of the *Available Power* we numerically traversed the imaginary downstream turbine through 50 different offset positions from $z/D = [-0.50, +0.50]$ allowing a location of the wake deflection with an accuracy of $\Delta z/D \approx 0.02$. An experimental validation with a comparable accuracy would be extremely elaborate or require an automatic traversing mechanism of the downstream turbine.
We therefore consider the presented comparison to serve as a general demonstration, but not as a sufficient validation of the *Available Power method*. We deem this demonstration not to add specific value to the discussion of our results and therefore suggest not to include this discussion in the manuscript.

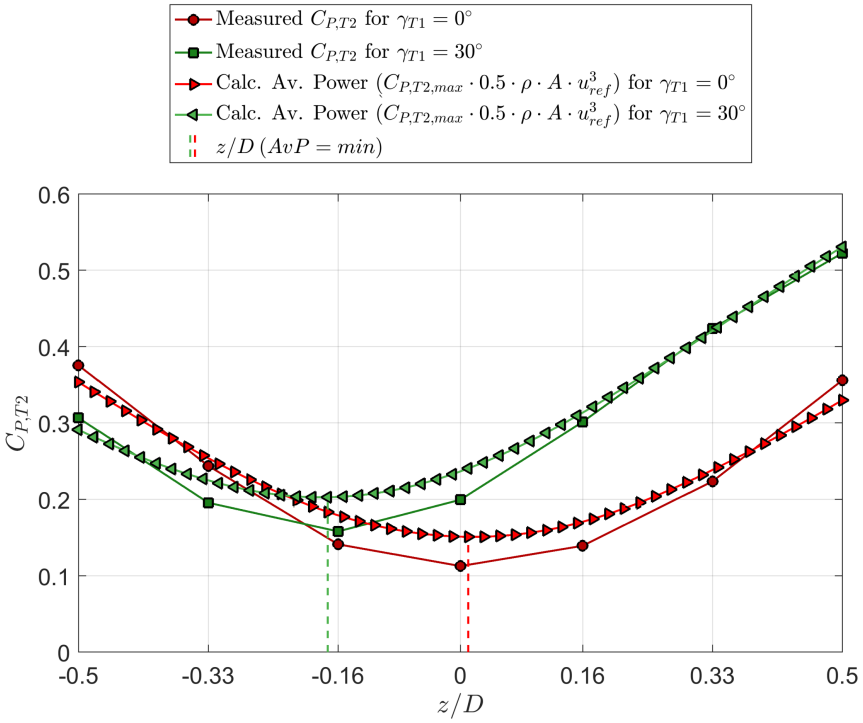

Figure 1: Comparison of the *Available Power* calculated from mean streamwise velocity distribution in the wake with the actually measured power of an identical downstream rotor traversed through the wake at $x/D = 3$ for inflow B. The *Available Power* in an imaginary rotor swept area A traversed through the wake is multiplied with the maximum downstream turbine power coefficient $C_{P,T2,max} = C_{P,T1,max} = 0.467$. Vertical dashed lines indicate z/D locations of the minimum calculated *Available Power*.

Specific comment (1)

The introduction is well done, with a good review of the literature to date. Useful to read it summarized in this way.

Thank you! We consider adding two new references by Fleming et al. (2017) and Berdowski et al. (2018) in the introduction of the final manuscript, as some interesting new research on this topic was published in the meanwhile.

p.2, l.29 ff:

The topic of utilizing yaw misalignment for improved wind farm control was thoroughly investigated by Fleming et al. (2015) and Gebraad et al. (2016). They analyzed wake mitigation strategies by using both a parametric wake model and the advanced computational fluid dynamics (CFD) tool SOWFA. A recent follow-up study by Fleming et al. (2017) focused on large-scale flow structures in the wake behind one and multiple aligned turbines and addresses a wake deflection behind a non-yawed downstream impinged by a partial wake of a yawed upstream turbine.

p.3, l.4 ff:

A combined experimental and computational wake study for a larger range of downstream distances was recently reported by Howland et al. (2016). The wake behind a yawed small drag disc of D=0.03 m was analyzed, describing the formation of a curled wake shape by a counter-rotating vortex pair. The influence of wake swirl, ground effect and turbulent diffusion on the formation mechanisms of this counter-rotating vortex pair was recently systematically investigated by Berdowski et al. (2018) using a free-wake vortex filament method.

Specific comment (2)

The selection of y as vertical and z as cross-wise was surprising to me, although since you provide a coordinate system in Fig 4., not too confusing. But is there a reason for this? FAST and Bladed for example both have z directed upward

This is a legitimate comment. Despite the unfortunate inconsistency of the coordinate system with most other publications and computational codes, we think that it is important to be consistent with our earlier publications (e.g. Bartl and Sætran (2017), Schottler et al. (2017b), Schottler et al. (2018)). We therefore carefully define the coordinate system in a clear sketch (Fig. 4 of the manuscript) before going into the results.

Specific comment (3)

Page 6, cos cubed is found for power-loss function. Anecdotally, this would be high for a utility-scale turbine I believe (although it fits the theoretical value). Is this a function of the scaling?

Thank you for this very good comment. It seems that a number of different values for the exponent x in the power-loss function $P(\gamma) = P_{max} \times cos^x$ have been found for different turbines of different sizes in different studies. This issue has amongst others been discussed in a thesis by Schepers (2012) as well as a review paper on yaw aerodynamics by Micallef and Sant (2016).
While earlier wind tunnel measurements at NTNU on the same rotor by Krogstad and Adaramola (2012) also find an exponent of $x = 3$, *"other measurements by Dahlberg and Montgomery (2005) found the exponent x to vary between 1.88 and 5.14"* (re-cited from Schepers, 2012). In 2001, Schepers further investigated this with another set of wind tunnel measurements and found an exponent of $x = 1.8$ (Schepers, 2001), which is significantly lower than the exponent found at NTNU.
It might be guessed that the exponent x could also be dependent on wind tunnel wall blockage, as blockage ($\sigma = 12.8\%$) significantly influences the power characteristics of the NTNU rotor. Measurements on a downscaled NTNU rotor ($D_{NTNU,small} = 0.45m$), however, confirm a power-loss-coefficient of about $x = 3$ (Bartl et al., 2018).
As stated by Micallef and Sant (2016), the exponent is deemed to be dependent on the induction distribution of the rotor. Therefore, a dependency of the exponent on the specific rotor design is assumed to be the main reason for the significant variations in the different experiments. A dedicated experiment on the power's yaw-dependency for different induction settings (e.g. through additional pitch or tip speed ratio variations) could help to further clarify this issue.

Specific comment (4)

Fig 11: I didn't understand why for the lower plots, two different methods of fitting are used. It had the impact on me, to reemphasize the difference in value of the points, since on the right the higher points are outliers to the fit.

Thank you for this good comment. We agree that the original version of Fig.11 was confusing. We assume that the values of the dotted lines in the lower left plot of the original version Fig. 11 in the manuscript might have been misunderstood. The single points shown in this subplot were the measured values of k/u_{ref}^2 for $\gamma = 0°$. These values were then multiplied with $cos(\gamma)^2$, which was found to be a good first order approximation for the turbulence levels for a yawed operation (shown as chain-dotted lines in the new plot). These locations of these reduced peak turbulence values are then scaled with a $\mu \pm \sigma_u$ approximation (derived from single Gaussian fits of the mean velocity profiles) and transferred to the lower right plot. There, the approximated values are again compared with measured values (for $\gamma = 30°$). The whole procedure shall demonstrate that it is possible to approximate the turbulence profile in the wake of a yawed turbine, when the turbulence profile of a non-yawed turbine and mean velocity profile behind the yawed turbine are known.
For a clearer presentation of this procedure, a new version of Fig. 11 in the manuscript (Fig. 2 in this document) is suggested, only including a single Gaussian fit of the velocity profiles. All other multiple-fitted curves are omitted. Additionally, small changes in the caption and text are suggested to also make the description clearer:

p.17, l.18 ff:

~~Effects of yawing on~~ Approximation for turbulent kinetic energy distributions in yaw

The levels of peak turbulence are observed to decrease considerably when the rotor is yawed. For a direct case-to-case comparison, TKE-profiles at hub height y=0 at x/D=6 are presented for $\gamma = 0°$ and $\gamma = -30°$ in the lower plots of Figure 11.

For a yawed turbine, the rotor thrust reduces with approximately $cos^2(\gamma)$ as previously shown in Figure 3. Multiplying also the TKE levels generated by the non-yawed rotor with $cos^2(\gamma)$ is observed to result in a decent first order approximation of the turbulence levels behind the yawed rotor. The reduced TKE levels for $\gamma = -30°$ are indicated by the chain-dotted lines in the lower left plot of Figure 11. ~~In order to also find~~For an approximation of the lateral deflection of the turbulence peaks for yawed rotors, ~~another first order approximation of~~their location can be estimated as proposed by Schottler et al. (2018)~~ is applied~~. In this approach the expected value and standard deviation of ~~the fitted~~ a Gaussian fit of the velocity profile behind a yawed rotor is calculated. Adding the standard deviation to the expected value $\mu \pm \sigma_u$ gives a rough estimate of the ~~corresponding TKE peak~~locations of the corresponding TKE peaks, as shown by the vertical ~~dashed~~lines in Figure 11. Thus, it is possible to ~~rescale the~~ approximate both TKE peak locations and levels by knowing TKE and mean velocity for the now-yawed case.

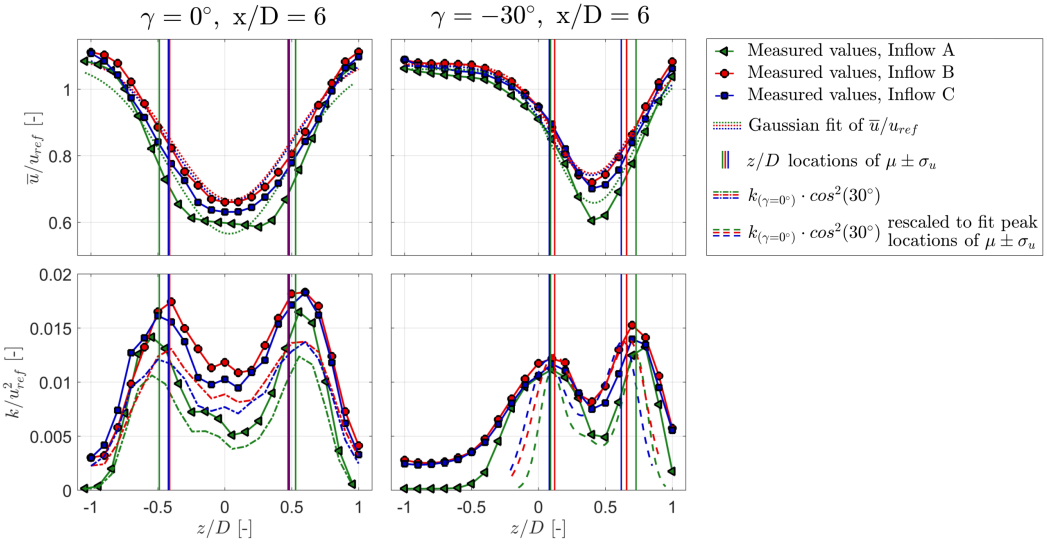

Figure 2: **Suggested simplified version of Figure 11:** Normalized mean velocity and turbulent kinetic energy k/u_{ref}^2 profiles at hub height $y = 0$ and x/D=6. The yaw angles are set to $\gamma = 0°$ and $\gamma = -30°$. Vertical lines indicate the borders of standard deviations of Gaussian-fitted velocity profiles $\mu \pm \sigma_u$. Chain-dotted lines indicate a TKE profiles at $\gamma = 0°$ multiplied by $cos^2(-30°)$. Dashed lines in the lower right subplot have the same magnitude as the chain-dotted lines, but are linearly scaled in z to fit the peak locations of $\mu \pm \sigma_u$.

Comment on connection to the companion paper:
I also could use a little more explanation of which material has been put into which paper and why. For example, the companion paper is focused on changes in TKE, and wind speed variability. Does it make sense to also discuss TI in this paper? To be clear, I am fine with the current division, but it would be helpful to understand a little more the distinction between the papers, if they both include profiles of turbulence for example. Perhaps one additional paragraph more explicitly delineating the papers, to be added to both?

Thank you for pointing this out. Most of this answer has been addressed in the answers to referee 1's comments of the companion paper already, but we repeat some of the main thoughts here.
In general, we deem the discussion of the rotor-generated TKE to be important for both papers. The TKE is separately discussed in each paper dependent on the different parameter variations performed.
The companion paper by Schottler et al. (2018) compares the wake flow behind two different model turbines. Therefore, the rotor geometry is the main parameter varied and investigated. The discussion of the TKE in the companion paper is important as it shows that the definition of the wake-width is very much dependent on which flow-parameter it is referred to. Comparing the three investigated wake flow parameters (1) mean velocity deficit, (2) TKE and (3) intermittency parameter λ^2 the affected area becomes significantly larger from (1) to (2) to (3).
In contrast to that, the present paper focuses on the impact of different inflow conditions on the wake flow and also the rotor-generated TKE in the wake. As the rotor-generated TKE in the wake can cause increased fatigue loads on potential downstream turbines, this parameter's inflow dependency is deemed important to be investigated.
As stated in the answer to the referees comments in the companion paper, we suggest to add another sentence to the introduction in order to make a more clear distinction between the papers:

p. 3, ll. 1 ff.
This work is part of a joint experimental campaign by the NTNU in Trondheim and ForWind in Oldenburg. ~~A~~ While this paper examines the influence of varying inflow conditions on the wake of one model wind turbine, a second paper by Schottler et al. (2018) compares the wake characteristics behind two different model wind turbines during exposed to one inflow only while also adding two-point statistics to the evaluation.

References

[1] Schottler, J., Hölling, A., Peinke, J., and Hölling, M.: Brief communication: On the influence of vertical wind shear on the combined power output of two model wind turbines in yaw, Wind Energy Science, 2, 439–442, doi: 10.5194/wes-2-439-2017, 2017a.

[2] Vollmer, L., Steinfeld, G., Heinemann, D., and Kühn, M.: Estimating the wake deflection downstream of a wind turbine in different atmospheric stabilities: an LES study, Wind Energy Science, 1, 129–141, doi: 10.5194/wes-1-129-2016, 2016.

[3] Fleming, P., Gebraad, P. M., Lee, S., van Wingerden, J.-W., Johnson, K., Churchfield, M., Michalakes, J., Spalart, P., and Moriarty, P.: Simulation comparison of wake mitigation control strategies for a two-turbine case, Wind Energy, 18, 2135–2143, doi: 10.1002/we.1810, 2015.

[4] Fleming, P., Annoni, J., Churchfield, M., Martinez, L., Gruchalla, K., Lawson, M., and Moriarty, P.: From wake steering to flow control, Wind Energ. Sci. Disc., doi: 10.5194/wes-2017-52, 2017.

[5] Sarlak, H., Nishino, T., Martinez-Tossas, L.A., Meneveau, C., and Sørensen, J.N.: Assessment of blockage effects on the wake characteristics and power of wind turbines, Renewable Energy 93, 340–352, doi: 10.1016/j.renene.2016.01.101, 2016.

[6] Schottler, J., Bartl, J., Mühle, F., Sætran, L., Peinke, J., and Hölling, M.: Wind tunnel experiments on wind turbine wakes in yaw: Redefining the wake width, Wind Energy Science Discussions, doi: 10.5194/wes-2017-58, 2018.

[7] Bartl, J., Müller, A., Landolt, A., Mühle, F., Vatn, M., Oggiano, L., and Sætran, L.: Validation of the real-time-response ProCap measurement system for full field flow measurements in a model-scale wind turbine wake, Manuscript submitted to Journal of Physics: Conference Series, DeepWind 2018 Conference, 2018.

[8] Pierella, F. and Sætran, L.: Wind tunnel investigation on the effect of the turbine tower on wind turbines wake symmetry, Wind Energy, 20, 1753-–1769, doi: 10.1002/we.2120, 2017.

[9] Jonkman, J., Butterfield, S., Musial, W. and Scott, G.: Definition of a 5-MW Reference Wind Turbine for Offshore System Development, Technical Report NREL/TP-500-38060, 2009.

[10] Schlichting, H.: Boundary layer theory, McGraw-Hill, 1986.

[11] Berdowski, T., Ferreira, C. van Zuijlen, A. and van Bussel, G.: Three-Dimensional Free-Wake Vortex Simulations of an Actuator Disc in Yaw, AIAA SciTech Forum, Wind Energy Synopsium 2018, doi: 10.2514/6.2018-0513, 2018.

[12] Bartl, J. and Sætran, L.: Blind test comparison of the performance and wake flow between two in-line wind turbines exposed to different turbulent inflow conditions, Wind Energ. Sci., 2, 55–76, doi: 10.5194/wes-2-55-2017, 2017.

[13] Schottler, J., Mühle, F., Bartl, J., Peinke, J., Adaramola, M.S., Sætran, L. and Hölling, M.: Comparative study on the wake deflection behind yawed wind turbine models, Journal of Physics: Conference Series, Volume 854, doi: 10.1088/1742-6596/854/1/012032, 2017b.

[14] Schepers, J.G.: Engineering models in wind energy aerodynamics, PhD thesis TU Delft, ISBN: 978-94-6191-507-8, 2012.

[15] Micallef, D. and Sant, T.: A Review of Wind Turbine Yaw Aerodynamics, Intech, doi: 10.5772/63445, 2016.

[16] Krogstad, P.-Å. and Adaramola, M. S.: Performance and near wake measurements of a model horizontal axis wind turbine, Wind Energy, 15, 743–756, doi: 10.1002/we.502, 2012.

[17] Dahlberg J.A. and Montgomerie B.: Research program of the Utgrunden Demonstration Offshore Wind Farm, Final report Part 2, Wake effects and other loads. FOI 2005-02-17, Swedish Defense Research Agency, FO, 2005.

[18] Schepers, J.G.: EU project in German Dutch Wind Tunnel. ECN-RX– 01-006, Energy Research Center of the Netherlands, ECN, 2001.

Authors' response to Referee #2:

We would like to thank the referee for reviewing this manuscript, the valuable feedback and the very constructive comments. At this stage of the review process, we respond to the referee #2's comments and propose improvements for the final manuscript. The referee's original comments are printed in **bold** followed by the corresponding answers. Passages from the manuscript are printed in *italic writing*, in which proposed additions are indicated in blue and deleted parts in ~~red~~.
Thank you very much for your efforts,

Jan Bartl on behalf of all authors

Content-related remark (1)

In the introduction, p1.l20, you state wake redirection techniques, which intentionally apply an uneven load distribution. Instead of an uneven loading, I would say that key to wake steering is the tilting of the thrust vector. For instance, cyclic pitching results is a large uneven loading, but marginal steering, while yaw results in a much smaller uneven loading, but a large thrust vector tilting.

Thank you for the good comment. In our understanding a tilted thrust vector and an uneven rotor load distribution (or *uneven distribution of induction*, (Micallef and Sant, 2016)) are a direct consequence of each other. Intuitively, cyclic pitching results in an uneven (cyclic) rotor loading, which then causes an unevenly distributed thrust over the rotor plane (not tilted but varying in magnitude) and consequently a tilt or yaw moment. During yaw misalignment, the thrust vector is laterally tilted, creating a yaw moment and consequently uneven rotor loads.

This is in agreement with a description by Fleming et al (2014.):
During yaw misalignment *(...) the thrust force of the turbine is shown to act along the axis of the rotor shaft. When the wind inflow is at an angle to this direction, the thrust can be divided into components fx and fy. The component fx is parallel to the flow and slows the wind, while fy is perpendicular and applies the force that causes wake redirection. IPC creates an uneven distribution of thrust forces on the rotor blades over the course of a rotation (...). This creates a tilt or yaw moment on the turbine rotor. (...) Therefore the in-plane reaction forces of the rotor on the flow are also unbalanced resulting in the fact that the turbine applies a net force on the flow perpendicular to the thrust direction, which does cause the flow to be redirected and the wake structure to be skewed.*

We do however agree that *a tilted thrust vector* intuitively is a better description for the causes of wake redirection in the context of yaw misalignment. We therefore suggest the following small modification in the manuscript:

p.1, l.19 ff:

These methods include the reduction of the upstream turbine's axial-induction by varying its torque or blade pitch angle (Annoni et al., 2016; Bartl and Sætran, 2016) as well as wake redirection techniques, which intentionally apply ~~an uneven load distribution~~ a tilted thrust vector on the front row rotors. In Fleming et al. (2015) different wake deflection mechanisms have been discussed with respect to higher wind farm power production and rotor loads.

Content-related remark (2)

On page 11, in the subsection about the tower wake deflection, you discuss several factors that contribute to the tower shadow deflection. You mention the influence of the lateral offset between the rotor and the tower during yawing, and the effect of the CVP (Counter-rotating Vortex Pair) on the wake opposite tower wake direction. What I suspect here is that the bottom of the two counter-rotating vortices is in strong interaction with its mirror image underground (i.e. the ground effect), thereby forming another CVP, but in opposite direction to the main CVP involved in the wake steering. This could hypothetically boost the deflection of the wake shadow in opposite direction to the main wake deflection.

Thank you for this very interesting comment. We agree that the lateral offset between the rotor midpoint (center of yaw rotation) and the tower midpoint might only play a minor role in the significant deflection of the tower wake as shown in e.g. Figure 6 (a) of the manuscript. The main contribution is deemed to stem from a strong cross flow (caused by the lower vortex of the CVP) near the ground as shown in Figure 6 (b) of the manuscript.
The formation of another CVP due to the interaction with the ground as seen in Bastankhah and Porte-Agel (2016) or Berdowski et al. (2018), is not directly observed in our experimental study. An analysis of the streamwise vorticity ω_x in Figure 6 (c) of the manuscript does not clearly show the formation of another CVP near the ground. As discussed in detail in the answers to **Content-related remark (5)** later in this document, the ground effect is deemed not to play a significant role in our wind tunnel experiment. Apart from the tower, our setup is perfectly symmetrical, featuring the same distance of the rotor to the floor and the roof of the closed wind tunnel cross-section.
For a clearer distinction of the effects of the tower wake deflection, we suggest the following small additions to the text:

p.11, l.16 ff:

On the bottom of the wake contour plot~~s~~ in Figure 6 (a), the wake of the turbine tower is indicated. The tower wake is observed to be deflected in the opposite direction than the rotor wake when the turbine is yawed. The deflection of the tower wake in the opposite direction is believed to have two reasons. Firstly, the turbine tower has a slight offset from $z/D = 0$ as the center of yaw-rotation was set to the rotor midpoint and not the tower. Therefore, a minor offset from the central position is expected

for the tower wake. Secondly and more importantly, the tower wake experiences an additional deflection in opposite direction due to an adversely directed cross-flow component outside near the wind tunnel floor as depicted in the vector plot in (Figure 6 (b)). This cross-flow balances the counter-rotating vortex pair above and possibly deflects the tower wake further to the side.

Content-related remark (3)

On page 12, the insignificant influence of the moderately sheared inflow on the wake shape is addressed. However, this can only be stated about the shear inflow under high turbulence conditions, as that is the only case you analysed. It might be the case that shear does have a significant contribution for low ambient turbulence levels, as the inflow shear in combination with the wake shear results in a distinctively high velocity gradient near the top of the wake (as shown by many researchers), thus increasing turbulence levels there. By the way, you mention this notion in the discussion about the TKE results later on in the paper.

Thank you for this very good comment. We do completely agree that the insignificant influence of the moderately sheared inflow on the wake only holds for the investigated highly turbulent inflow. This situation might not be very realistic, as in reality stronger vertical flow gradients are mostly present in stable atmospheric conditions featuring a low ambient turbulence level (Vollmer et al., 2016). However, it is very difficult to create a low-turbulent sheared inflow in a wind tunnel experiment with a limited wind tunnel length.
We agree that we have to be clearer about this at two passages in the text, and therefore suggest the following additions:

p.1, l.6 f:
Exposing the rotor to non-uniform highly turbulent shear inflow changes the mean and turbulent wake characteristics only insignificantly.

p.10, l.25 f:
Despite the sheared inflow the wake shapes for all three yaw angles and both downstream distances are observed to be very similar to those of test case B. The normalized velocity levels as well as the inner structure of the wake are almost identical. The influence of shear is however only investigated at high inflow turbulence levels, which does not allow for any conclusions at lower inflow turbulence levels.

Content-related remark (4)

For completeness, it is important that the parameter settings for the JMC and BPA models is provided.

Thank you for pointing this out. The parameter settings are, of course, very important for the reproducibility of the deflection calculations. The recommended default

model-parameters were used in both cases. We suggest the following additions to the manuscript:

p.13, l.2 f:
Further, the results are compared with two different wake models by Jimenez et al. (2010) (JCM) and Bastankhah and Porte-Agel (2016) (BPA). The recommended default model-parameters were used in the implementation of both wake deflection models. For the JCM-model a linear wake expansion factor of $\beta = 0.125$ was applied, while $k_y = 0.022$, $k_z = 0.022$, $\alpha^* = 2.32$ and $\beta^* = 0.154$ were used in the case of the BPA-model. The comparisons of the wake deflections are shown in Figure 8.

Content-related remark (5)

On page 14, you note that the wake deflection of a non-yawed turbine is assumed to stem from the interaction of the rotating wake with the turbine tower. The fact that the wake of a counter-clockwise rotating turbine (thus with a clockwise rotating wake swirl) deflects in positive z direction, sounds to me as originating from the interaction between the wake swirl and the ground: the root vortex forms a CVP with its mirror image underground from the ground effect, with its deflection direction in positive z direction. This was also discussed by e.g. Fleming (2014) and BPA (2016).

This is a very good comment directed towards the core of manuscript, namely the asymmetrical interaction of the different vortices in the yawed wake. For a detailed discussion about the causes for an asymmetrical wake deflection it is also referred to the answers to **Overall comments (1b) and (1c)** in the **Authors' response to RC1**, in which a very similar comment was addressed.

The interaction of the ground with the counter-rotating vortex pair (CVP) in the wake of a yawed turbine has been discussed by Fleming et al. (2014), Bastankhah and Porte-Agel (2016) and Berdowski et al. (2018).
The study by Fleming et al. (2014) already discusses wake asymmetries influenced by the ground effect for a non-yawed turbine. *"The wake rotates counter-clockwise in these contour planes, i.e. opposite to the clockwise rotation of the turbine rotor, and the wake is like a vortex interacting with the ground. The clockwise-rotating image wake (when considering the ground plane as an image plane in potential flow) then induces motion on the actual wake, pushing it to the right."*
By the means of theoretical potential theory study Bastankhah and Porte-Agel (2016) observe a different *"wake-centre displacement (...) in both horizontal and vertical directions (...). This is due to the fact that the wake rotation and ground effects act against each other"* for one yaw direction, while they act in the same direction for the other yaw direction.
A recent computational free-wake vortex filament study by Berdowski et al. (2018) investigated the ground effect for a yawed actuator disc. In this study, ground effects could be isolated by running two different simulations, of which only one was including a symmetry plane on the ground. For this case they observed that *"the bottom vortex of the CVP forms another CVP with its mirror vortex underground and in opposite*

direction" (Berdowski et al., 2018).

The experimental setup investigated in this manuscript, however, is perfectly symmetrical, i.e. the rotor is located in the center of the wind tunnel, meaning that it has the same distance to wind tunnel floor and roof respectively the right and left sidewall. Our model turbine ($D \approx 90cm$) is installed with a hub height ($h_{hub,exp} = 89cm$) adjusted to the center of the wind tunnel ($h_{tunnel} \approx 180cm$), such that the setup is almost perfectly symmetrical. As shown in Fig. 6 (c) in the manuscript, we did not observe a formation of another CVP in our experimental setup.

As explained in the **Authors' response to RC1, Comment (1b)**, the effect of the tower wake on the rotor wake is deemed to be the main influence factor introducing asymmetries to the setup. However, the tower wake in this model scale experiment is deemed to be significantly stronger in the Reynolds-number-range of model-scale experiments than in full-scale situations. As this is a very critical issue, we suggest to add some more lines to the explanation on p.14 (as suggested in the answers to RC1 already):

p.14, l.5 ff:
The wake shows a higher deflection for negative yaw angles in all inflow cases. Also the wake behind the non-yawed turbine is seen to be slightly deflected in positive z-direction, which is assumed to stem from the interaction of the rotating wake with the turbine tower. As discussed by Pierella and Sætran (2017) who performed experiments on the same rotor with a slightly larger tower, the tower-wake interaction ~~can lead~~ leads to an uneven momentum entrainment in the wake. For the non-yawed case Pierella and Sætran (2017) observed both a lateral and vertical displacement of the wake vortex center, induced by an interaction with the tower wake. It can therefore be assumed that also the interaction of the counter-rotating vortex pair with the tower wake slightly displaced wake vortex in the yawed cases might be influence by an interaction with the tower wake, which is the only source of asymmetry in an otherwise perfectly symmetrical setup.

Content-related remark (6)

On page 14, you mention that the differences are small for the wake deflection as compared between a high and low turbulence inflow. Here it would be helpful to present results of the streamwise vorticity for both cases and for several downstream positions. Maybe the diffusion of vorticity under self-induced turbulence is already very significant for low ambient turbulence levels, which would explain why both cases are then so similar. In the end, the analysis of streamwise vorticity is key to understand, as the streamwise vorticity forms the CVP which is the driving force behind both the wake deflection and the shape deformation.

This is a very good idea for a deeper analysis. We agree the diffusion of vorticity in a field of rotor-generated turbulence for low inflow turbulence levels might be very

similar to that of higher inflow turbulence levels. However, a more detailed analysis would be needed to support this assumption.
Unfortunately, we are not able present and analyze the streamwise vorticity for all wake scans at this stage, as our Laser-Doppler-Anemometer (LDA) only allowed recording two velocity components at a time. We decided to record the streamwise component u and the vertical component v. For an assessment of the streamwise vorticity ω_x, also the lateral velocity component w would be needed. This component was additionally measured for one wake scan only, which included in the parameters presented in Figure 6 of the manuscript.
As the vorticity is deemed to be of major interest for an assessment of the different diffusion in the flow, we suggest to add a line one that issue in the discussion section of the manuscript, motivating a deeper analysis of this in future studies.

p.18, l.19:
Our study moreover indicates that the wake shape and deflection is affected by inflow turbulence. The overall wake deflection was observed to be similar for both investigated turbulence levels. For a more detailed investigation of diffusion mechanisms in the wake, however, a vorticity analysis in the wake of a turbine exposed to low and high turbulence is motivated for future studies. The inflow turbulence is furthermore implemented ~~This confirms the implementation of the inflow turbulence~~ as an input parameter in the recently developed wake model by Bastankhah and Porte-Agel (2016).

Content-related remark (7)

In figure 11, vertical lines of the standard deviation are given, but it is unclear how the mean and standard deviation are defined here. After all, the Gaussian fit curves applied here are clearly not symmetric, thus I assume those are from a fit with multiple Gaussians, for which it is less trivial to define a mean and standard deviation. Apart from that, there is a lot of information in this figure, and it took me a while to comprehend it fully.

Thank you for this good comment. We agree that Figure 11 of the manuscript can be misunderstood and needs to be simplified. The mean and the standard deviation are defined from a single Gaussian fit function of the mean velocity profile at hub height. Confusingly, this single Gaussian fit was not shown in the original version of Figure 11 of the manuscript. The original version included a couple of multiple Gaussian fits for the mean velocity and TKE profiles, which might have been misleading. For a clearer presentation, a new version of Figure 11 is suggested including the single Gaussian fit of the velocity profiles, while all other multiple-fitted curves are omitted. A suggested modified version of the manuscript's Fig. 11 is shown in Figure 2 of this answer document.
Additionally, small changes in the caption and text are suggested to also make the description clearer:

p.17, l.18 ff:

~~Effects of yawing on~~ Approximation for turbulent kinetic energy distributions in yaw

The levels of peak turbulence are observed to decrease considerably when the rotor is yawed. For a direct case-to-case comparison, TKE-profiles at hub height y=0 at x/D=6 are presented for $\gamma = 0°$ and $\gamma = -30°$ in the lower plots of Figure 11.

For a yawed turbine, the rotor thrust reduces with approximately $cos^2(\gamma)$ as previously shown in Figure 3. Multiplying also the TKE levels generated by the non-yawed rotor with $cos^2(\gamma)$ is observed to result in a decent first order approximation of the turbulence levels behind the yawed rotor. The reduced TKE levels for $\gamma = -30°$ are indicated by the chain-dotted lines in the lower left plot of Figure 11. ~~In order to also find~~For an approximation of the lateral deflection of the turbulence peaks for yawed rotors, ~~another first order approximation of~~their location can be estimated as proposed by Schottler et al. (2018)~~ is applied~~. In this approach the expected value and standard deviation of ~~the fitted~~ a Gaussian fit of the velocity profile behind a yawed rotor is calculated. Adding the standard deviation to the expected value $\mu \pm \sigma_u$ gives a rough estimate of the ~~corresponding TKE peak~~locations of the corresponding TKE peaks, as shown by the vertical ~~dashed~~lines in Figure 11. Thus, it is possible to ~~rescale the~~ approximate both TKE peak locations and levels by knowing TKE and mean velocity for the now-yawed case.

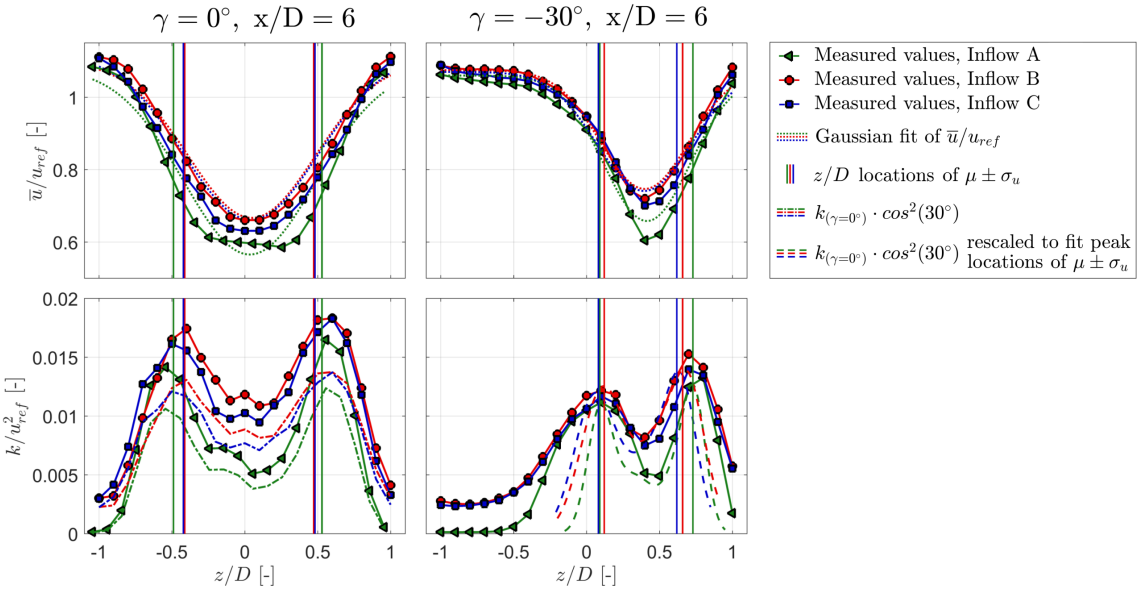

Figure 1: **Suggested simplified version of Figure 11:** Normalized mean velocity and turbulent kinetic energy k/u_{ref}^2 profiles at hub height $y = 0$ and x/D=6. The yaw angles are set to $\gamma = 0°$ and $\gamma = -30°$. Vertical lines indicate the borders of standard deviations of Gaussian-fitted velocity profiles $\mu \pm \sigma_u$. Chain-dotted lines indicate a TKE profiles at $\gamma = 0°$ multiplied by $cos^2(-30°)$. Dashed lines in the lower right subplot have the same magnitude as the chain-dotted lines, but are linearly scaled in z to fit the peak locations of $\mu \pm \sigma_u$.

Technical remark (1)

P3.l4 – "donstream" → "downstream"
P3.l24 – remove "used in"
P3.l27 – "a NREL" → "an NREL"
Table 1 – add full stop
Figure 2 – add full stop
Table 2 – "CT" → "C_T"
Table 2 – add full stop
P7.l3 – "a HBM" → "an HBM"
P8.l14 – "a eight" → "an eight"
P8.l16 – remove "these" before "all these"
P8.l16 – remove "as a result" (duplication with "is obtained")
P9.l22 – "an solid" → "a solid"
P11.l10 – add "been" in between "previously investigated"
P12.l13 – remove "in"
P13.l9 – add "the" before "BPA-model"
P13.l9 – lowercase for "Available"
P13.l16 – duplicate of the word "complex"
P13.l20 – "a input" → "an input"
P15.l13 – remove "and"
Figure 10 – add full stop
Figure 11 – remove "a" before "TKE profiles"
P18.l16 – "slight" → "slightly"
P19.l2 – "shown" → "show"

Thank you for indicating these technical errors. We corrected all of them in the revised version of the manuscript.

Technical remark (2)

Comma's could be used more extensively to increase readability. For instance, see the first paragraph of section 4.1: "At the top, the"; "As the rotor thrust is reduced, a"; "For a yawed rotor, a"; "Due to this lateral force component, the"; "Comparing the wake contours [: : :] , an asymmetry": : :

Thank you for pointing this out. Commas have been added at the suggested passages in the text. Special attention will be given to commas in a final proof-reading of the manuscript.

Technical remark (3)

Sometimes it would make the text more easily readable if the text would be broken up into several paragraphs. For instance, p13.l18: "Secondly, the wake: : :" is a confusing construction, as there is no "firstly" defined in your text. Moreover, this sentence refers to a new comparison, so to clarify the text it would be better to break it up into two sections.

This is indeed an incorrect use of the word "Secondly,...". We replaced it with "Further,..." in the revised version of the manuscript.

Technical remark (4)

At p2.l18, "The measured circulation in the wake showed clear asymmetries for positive and negative yaw angles". This is about the asymmetry of the wake regarding the kidney shape, but this sentence could also be read as an asymmetry between the values for positive and negative yaw (i.e. yaw dependency).

We agree that the wording of the addressed sentence is equivocal. We therefore suggest a clearer wording:

p.2, l.17 ff:
In a follow-up study, Grant and Parkin (2000) presented phase-locked particle image velocimetry (PIV) measurements in the wake. The measured circulation in the wake showed clear asymmetries in the wake shape for positive and negative yaw angles.

Technical remark (5)

In figure 1, a clockwise rotating turbine is presented in the left subfigure, while the other two subfigures depict an anti-clockwise rotating turbine. Although it was clearly mentioned in the text that the results were for a turbine that is anti-clockwise rotating, it was a bit confusing for me at first to see the picture for the clockwise rotating turbine (which I assume is the second turbine used for the experiments later on in the paper).

Well observed. The rotor depicted in Figure 1.(a) of the manuscript turns clockwise and therefore is wrong in this setting. We updated the figure with a counter-clockwise turning rotor as shown in Figure 2, which now should be correct.

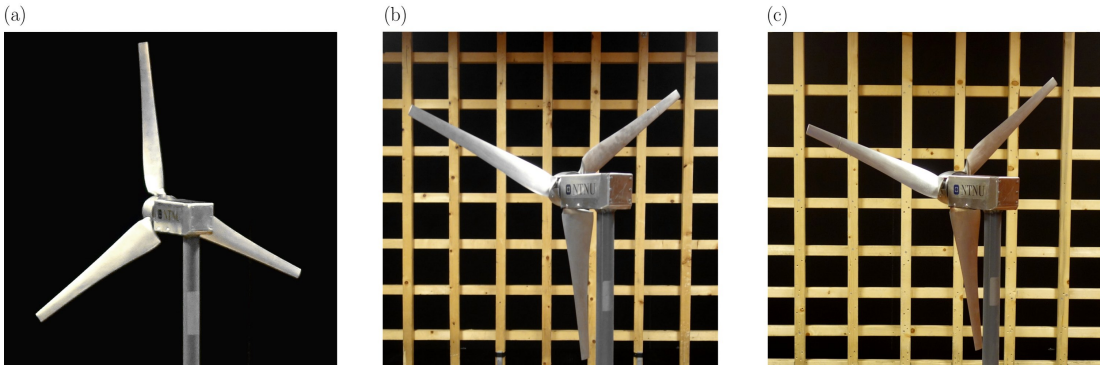

Figure 2: Yawed model wind turbine exposed to different inflow conditions: **(a)** $TI_A = 0.23\%$, uniform **(b)** $TI_B = 10.0\%$, uniform **(c)** $TI_C = 10.0\%$, non-uniform shear.

Technical remark (6)

At page 6, it would be good to add the approximate values for cos2(30) and cos3(30) in the main text to get a feeling for their magnitude (0.75 and 0.65 respectively).

That is a good idea. Although the approximated and actually measured values already are compared in Figure 3 of the manuscript, the approximated values are never mentioned in the text. For a value-to-value comparison with the measured $C_{P/T,\gamma=30}$ as presented in Table 2 of the manuscript, we propose the following small additions to the text:

p.6, l.12 ff:
An approximation of this reduction can be obtained with sufficient accuracy by multiplying the maximum power of the non-yawed turbine by $C_{P,A}{\cdot}cos^3(30°) \approx 0.304$. *An adequate estimate of the thrust coefficient of the yawed rotor can be obtained assuming a reduction by* $C_{T,A}{\cdot}cos^2(30°) \approx 0.670$ *on the thrust of the non-yawed rotor. This corresponds well to previous measurements by Krogstad and Adaramola (2012).*

Technical remark (7)

In figure 5 you apply a very fine gradient scaling with contour lines added, but it is hard to extract the true magnitude from these plots. You might change these plots to one where you have much fewer gradient colors (let's say about 10), and change the colorbar accordingly (which is completely smooth in the current visualization).

Thank you for this good comment. Matlab offers a number of different pre-defined and the option for custom defined colormaps. The most commonly used pre-defined maps are "jet" and "parula". "Jet" offers a wider spectrum of colors, which makes it easier to extract the magnitude of the values from a plot. "Parula", on the other hand, appears more linear to the eye. We therefore decided to plot our wake results using the "parula" colormap.
We deem it is very important that the colormaps are consistent with our earlier publications (e.g. Bartl et al. (2017), Schottler et al. (2018)) and therefore propose to keep the colormaps as they are in the manuscript. However, we now made all our experimental wake data publicly available on a web-platform including a digital object identifier (doi). This enables everyone to download the wake data and adjust the colormaps according to their specific preferences. We propose to add a short line called *"Data availability"* in the end of the manuscript:

p.19, l.26:
Data availability. All presented wake data in this paper is available on *https://doi.org/10.5281/zenodo.1193656* .

Technical remark (8)

In section 4.1, the subsection about the curled wake shape, you mention ": : : a kidneyshaped velocity deficit is observed: : :", without referring to a figure number. The same applies for the subsection about the tower wake deflection on the next page.

Thank you for pointing this out. We suggest to add a reference to the specific figures in both cases:

p.10, l.32:
At x/D=6 a kidney-shaped velocity deficit is observed (Figure 5), showing a higher local velocities behind the rotor center.

p.11, l.16:
On the bottom of the wake contour plots in Figure 6 (a), the wake of the turbine tower is indicated.

Technical remark (9)

In general, it comes more natural for the understanding of the reader if the lateral direction was defined as y and the vertical direction as z instead.

This is a legitimate comment, which has also been addressed by referee 1. Despite the unfortunate inconsistency of our coordinate system with most other definitions, we think that it is important to be consistent with our earlier publications (e.g. Bartl and Sætran (2017), Schottler et al. (2017), Schottler et al. (2018)). We therefore carefully define the coordinate system in a clear sketch (Fig. 4 of the manuscript) before going into the results.

References

[1] Micallef, D. and Sant, T.: A Review of Wind Turbine Yaw Aerodynamics, Intech, doi: 10.5772/63445, 2016.

[2] Fleming, P., Gebraad, P. M., Lee, S., van Wingerden, J.-W., Johnson, K., Churchfield, M., Michalakes, J., Spalart, P., and Moriarty, P.: Evaluating techniques for redirecting turbine wakes using SOWFA, Renewable Energy, 70, 211–218, doi: 10.1016/j.renene.2014.02.015, 2014.

[3] Bastankhah, M. and Porté-Agel, F.: Experimental and theoretical study of wind turbine wakes in yawed conditions, Journal of Fluid Mechanics, 806, 506–541, doi: 10.1017/jfm.2016.595, 2016.

[4] Berdowski, T., Ferreira, C. van Zuijlen, A. and van Bussel, G.: Three-Dimensional Free-Wake Vortex Simulations of an Actuator Disc in Yaw, AIAA SciTech Forum, Wind Energy Synopsium 2018, doi: 10.2514/6.2018-0513, 2018.

[5] Pierella, F. and Sætran, L.: Wind tunnel investigation on the effect of the turbine tower on wind turbines wake symmetry, Wind Energy, 20, 1753-–1769, doi: 10.1002/we.2120, 2017.

[6] Vollmer, L., Steinfeld, G., Heinemann, D., and Kühn, M.: Estimating the wake deflection downstream of a wind turbine in different atmospheric stabilities: an LES study, Wind Energy Science, 1, 129–141, doi: 10.5194/wes-1-129-2016, 2016.

[7] Schottler, J., Bartl, J., Mühle, F., Sætran, L., Peinke, J., and Hölling, M.: Wind tunnel experiments on wind turbine wakes in yaw: Redefining the wake width, Wind Energy Science Discussions, doi: 10.5194/wes-2017-58, 2018.

[8] Bartl, J. Ostovan, Y., Uzol, O. and Sætran, L.: Experimental study on power curtailment of three in-line turbines, Energy Procedia, vol. 137C, pp. 307-314, doi: 10.1016/j.egypro.2017.10.355, 2017.

[9] Bartl, J. and Sætran, L.: Blind test comparison of the performance and wake flow between two in-line wind turbines exposed to different turbulent inflow conditions, Wind Energ. Sci., 2, 55–76, doi: 10.5194/wes-2-55-2017, 2017.

[10] Schottler, J., Mühle, F., Bartl, J., Peinke, J., Adaramola, M.S., Sætran, L. and Hölling, M.: Comparative study on the wake deflection behind yawed wind turbine models, Journal of Physics: Conference Series, Volume 854, doi: 10.1088/1742-6596/854/1/012032, 2017b.

Wind tunnel experiments on wind turbine wakes in yaw: Effects of inflow turbulence and shear

Jan Bartl[1], Franz Mühle[2], Jannik Schottler[3], Lars Sætran[1], Joachim Peinke[3,4], Muyiwa Adaramola[2], and Michael Hölling[3]

[1] Department of Energy and Process Engineering, Norwegian University of Science And Technology, Trondheim, Norway
[2] Faculty of Environmental Sciences and Natural Resource Management, Norwegian University of Life Sciences, Ås, Norway
[3] ForWind, Institute of Physics, University of Oldenburg, Oldenburg, Germany
[4] Fraunhofer IWES, Oldenburg, Germany

Correspondence to: Jan Bartl (jan.bartl@ntnu.no)

Abstract. The wake characteristics behind a yawed model wind turbine exposed to different customized inflow conditions are investigated. Laser Doppler Anemometry is used to measure the wake flow in two planes at x/D=3 and x/D=6 while the turbine yaw angle is varied from $\gamma = [-30°, 0°, +30°]$. The objective is to assess the influence of grid-generated inflow turbulence and shear on the mean and turbulent flow components.

The wake flow is observed to be asymmetric with respect to negative and positive yaw angles. A counter-rotating vortex pair is detected creating a kidney-shaped velocity deficit for all inflow conditions. Exposing the rotor to non-uniform highly turbulent shear inflow changes the mean and turbulent wake characteristics only insignificantly. At low inflow turbulence the curled wake shape and wake center deflection are more pronounced than at high inflow turbulence. For a yawed turbine the rotor-generated turbulence profiles peak in regions of strong mean velocity gradients, while the levels of peak turbulence decrease at approximately the same rate as the rotor thrust.

1 Introduction

In the light of a steadily increasing worldwide use of wind energy, optimized control for wind farms has become a focus area of research. The reduced wind speeds in the wake leave significantly less energy for downstream turbines causing wind farm power losses up to 20% (Barthelmie et al., 2010). At the same time increased turbulence levels in the wake lead to higher fatigue loads on downstream rotors, which experience an increased probability for component failure (Thomsen and Sørensen, 1999). In order to mitigate these unfavorable consequences of wake impingement, different wind farm control methods have been suggested for optimizing the total power output and minimizing loads on a wind farm's individual turbines (Knudsen et al., 2014; Gebraad et al., 2015).

These methods include the reduction of the upstream turbine's axial-induction by varying its torque or blade pitch angle (Annoni et al., 2016; Bartl and Sætran, 2016) as well as wake redirection techniques, which intentionally apply a tilted thrust vector on the front row rotors. In Fleming et al. (2015) different wake deflection mechanisms have been discussed with respect to higher wind farm power production and rotor loads. As individual pitch control has been shown to cause high structural

loads and current turbine designs do not feature a degree of freedom in tilt direction, yaw actuation has been concluded to be a very promising technique.

For the development of wake deflection strategies by yaw misalignment, the characteristics of the mean and turbulent wake flow behind a yawed turbine have to be understood in detail. Besides the turbine's geometry and operational state, the wake flow is strongly dependent on the atmospheric conditions which represent the inflow state to the turbine. The stability of the atmospheric boundary layer can be described by height-dependent distributions of potential temperature, wind direction (veer), velocity distribution (shear) and turbulence intensity (Vollmer et al., 2016). As it is rather impossible to simulate realistic atmospheric conditions in a wind tunnel environment, these parameters have to be investigated separately. Therefore, the present study investigates the dependency of the wake flow behind yawed turbines for different customized inflow conditions. The wind tunnel study intends to shed light on the effects of non-uniform shear and inflow turbulence levels on the wake characteristics. Wind tunnel wake experiments have the advantage of being conducted in controlled laboratory environment. Thus, intentional variations of inflow conditions and turbine operating points can help to gain a deeper understanding of the effects on the wake flow. They furthermore can serve as validation data of numerical results and a base for the fine-tuning of engineering wake models.

An early set of experimental studies on the wake of a yawed turbine was reported by Grant et al. (1997), in which they used optical methods in the wake behind a model turbine of D=0.90 m to track the tip vortices and calculate wake deflection and expansion. In a follow-up study, Grant and Parkin (2000) presented phase-locked particle image velocimetry (PIV) measurements in the wake. The measured circulation in the wake showed clear asymmetries in the wake shape for positive and negative yaw angles. An asymmetric wake was also reported by Haans et al. (2005), who found non-symmetric tip vortex locations behind a yawed model turbine of D=1.20 m. Another yaw experiment was conducted by Medici and Alfredsson (2006) on a small model turbine of D=0.12 m. They reported a clear cross-stream flow component deflecting the wake laterally. These experimental results were later used by Jiménez et al. (2010) as verification data for a wake deflection model for yawed turbines. Based on large eddy simulations (LES) around a yawed actuator disc they developed a simple analytical model that is able to predict the wake skew angle and wake velocity deficit in the far wake. An engineering model for the axial induced velocity on a yawed turbine was developed by Schepers (1999), which was based on inflow measurements in front of different yawed turbines.

An extensive study of flow and load characteristics on a yawed wind turbine rotor on a D=4.50 m rotor was presented by Schepers et al. (2014). In the so-called Mexnext project, a comparison of twenty different computations with detailed PIV and load measurements revealed modeling deficiencies while simultaneously shedding light on complex instationary flow at the rotor. The topic of utilizing yaw misalignment for improved wind farm control was thoroughly investigated by Fleming et al. (2015) and Gebraad et al. (2016). They analyzed wake mitigation strategies by using both a parametric wake model and the advanced computational fluid dynamics (CFD) tool SOWFA. A recent follow-up study by Fleming et al. (2017) focused on large-scale flow structures in the wake behind one and multiple aligned turbines and addresses a wake deflection behind a non-yawed downstream impinged by a partial wake of a yawed upstream turbine. In another LES investigation Vollmer et al. (2016) studied the influence of three atmospheric stability classes on the wake characteristics behind a yawed turbine rotor.

A strong dependency of the wake shape and deflection on the stability is found, showing significantly higher wake deflection for a stable atmosphere than for neutral or convective conditions. Another LES study on yaw misalignment was performed by Wang et al. (2017), who highlighted the importance of including nacelle and tower structures in the computational model when comparing with experimental results.

Yaw angle dependent turbine performance and near-wake measurements were performed by Krogstad and Adaramola (2012). They found a power decrease proportional to $cos^3(\gamma)$ and showed that the near-wake deflection is dependent on the turbine's tip speed ratio. A combined experimental and computational wake study for a larger range of downstream distances was recently reported by Howland et al. (2016). The wake behind a yawed small drag disc of D=0.03 m was analyzed, describing the formation of a curled wake shape by a counter-rotating vortex pair. The influence of wake swirl, ground effect and turbulent diffusion on the formation mechanisms of this counter-rotating vortex pair was systematically investigated by Berdowski et al. (2018) using a free-wake vortex filament method. An extensive contribution to the field of yawed turbine wakes was recently made by Bastankhah and Porté-Agel (2016). In an experimental PIV study on a model turbine of D=0.15 m an asymmetric flow entrainment in the wake by both mean and turbulent momentum fluxes was shown. Moreover, an analytical model for the far wake of a yawed turbine was developed based on self-similar velocity and skew angle distributions.

An experimental study on the interaction of two model wind turbines was conducted by Schottler et al. (2016) showing clear asymmetries of the downstream turbine power output with respect to the upstream turbine's positive or negative yaw angle. In a follow-up study the asymmetry was ascribed to a strong shear in the inflow, which caused an asymmetry in the opposite direction when the sheared inflow was vertically inverted (Schottler et al., 2017a). These studies encouraged a more detailed investigation of the inflow-dependent wake flow behind a yawed turbine. As for the present study, we aim to close the gap between turbine interactions for yaw-controlled wind farms by presenting high-fidelity wake measurement data at controlled inflow conditions. The influence of turbulence and shear in the inflow on the wake's shape, deflection and symmetry with respect to yaw angle is quantified. This work is part of a joint experimental campaign by the NTNU Trondheim and ForWind in Oldenburg. While this paper examines the influence of varying inflow conditions on the wake of one model wind turbine, a second paper by Schottler et al. (2018) compares the wake characteristics behind two different model wind turbines exposed to one inflow only while also adding two-point statistics to the evaluation.

2 Experimental setup

2.1 Turbine model, inflow & operating conditions

Turbine model

The wind turbine model used for this study has a rotor diameter of D=0.90 m with a hub diameter of D_{hub}=0.090 m. The tower and nacelle structure of the turbine is a slimmer re-design of the turbines previously used in Bartl and Sætran (2017). The tower thickness and the nacelle length have been significantly reduced in size in order to minimize their impact on the wake flow behind the yawed rotor. Photographs of the turbine exposed to different inflow conditions are shown in Figure 1. The blades are milled in aluminum and based on an NREL S826 airfoil, which was originally designed at the National Renewable

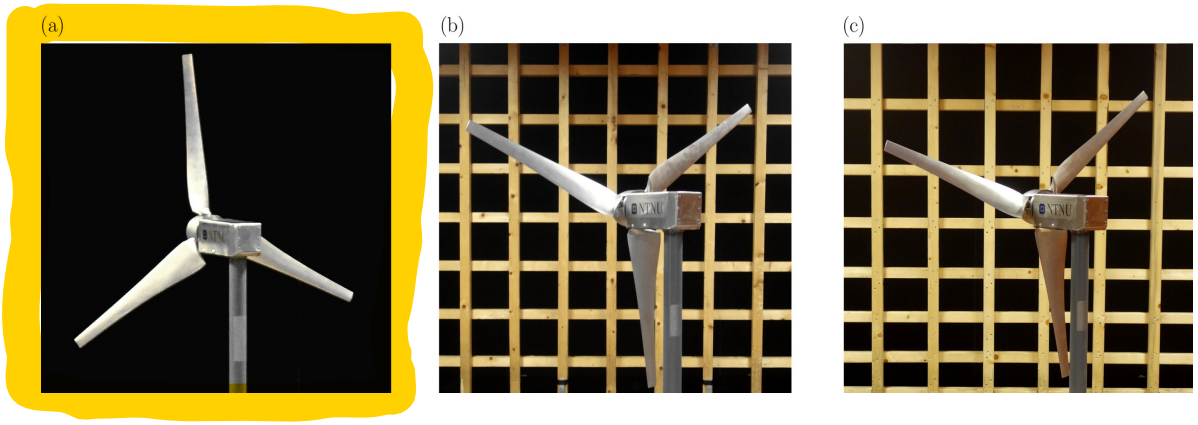

Figure 1. Yawed model wind turbine exposed to different inflow conditions: **(a)** TI_A=0.23%, uniform **(b)** TI_B=10.0%, uniform **(c)** TI_C=10.0%, non-uniform shear.

Energy Laboratory (NREL). The rotor turns in counter-clockwise direction when observed from an upstream point of view. The rotation is controlled via an electric servo motor of the type 400W Panasonic LIQI, which is located inside the nacelle. The frequency-controlled motor ensures a rotation at constant rotational speed, while the excessive power is burned off in an external resistor. The blade pitch angle was fixed to $\beta = 0°$ for the entire experiment.

Scaling and blockage

The experiments were performed at the low-speed wind tunnel at the Norwegian University of Science and Technology (NTNU) in Trondheim, Norway. The test section is $11.15\,\mathrm{m}$ long with an inlet cross-section of $2.71\,\mathrm{m} \times 1.81\,\mathrm{m}$ (width $\times$ height). Compared to a full scale wind turbine, the model size is scaled down at a geometrical scaling ratio of approximately 1:100 resulting in a mismatch in Reynolds number in the model experiment. The turbine is operated at a Reynolds number of approximately $Re_{\mathrm{tip}} \approx 10^5$ at the blade tip, which is more than one full order of magnitude lower than for full scale turbines. Re_{tip} is based on the chord length at the blade tip and the effective velocity during turbine operation.

Furthermore, the rotor swept area of the turbine model blocks 12.8 % of the wind tunnel's cross sectional area. The wind tunnel height is approximately twice the rotor diameter while its width measures about three times the diameter. Consequently, there is about one full diameter of space for lateral wake deflection on each side behind the rotor. However, an influence of the wind tunnel walls on the wake expansion and deflection cannot be completely excluded.

Inflow conditions

The measurements are performed for three different stationary inflow conditions as listed in Table 1. As shown in Figure 1 inflows B and C are generated by static grids at the inlet. The streamwise mean velocities and turbulence intensity levels mea-

Table 1. Characteristics of the three different investigated inflow conditions.

Inflow	TI [%]	spatial uniformity	power law coeff. α
A	0.23	uniform	0
B	10.0	uniform	0
C	10.0	non-uniform	0.11

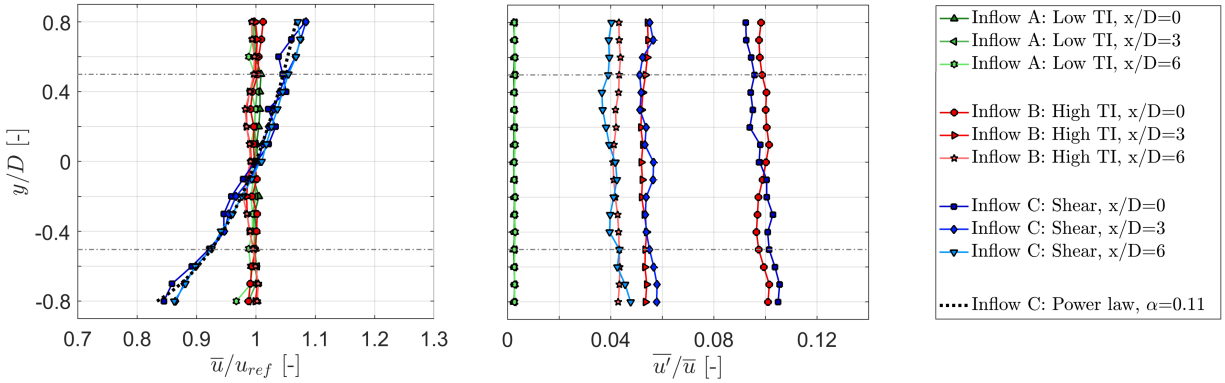

Figure 2. Normalized mean velocity $\overline{u}/u_{ref}$ and turbulence intensity $\overline{u'}/\overline{u}$ measured in the empty wind tunnel at the turbine position $x/D = 0$ and wake measurement positions $x/D = 3$ and $x/D = 6$.

sured in the empty wind tunnel at the turbine position (x/D=0) and wake measurement locations (x/D=3 and x/D=6) are presented in Figure 2.

Inflow A can be characterized as a typical laboratory flow, in which the turbine is exposed to the uniform, low turbulence inflow of the wind tunnel (TI_A=0.23%). The low turbulence level in test case A is considered to be far below the intensities present in the real atmospheric boundary layer. Nevertheless, test case A is considered an extreme test case for the performance of computational prediction models. In order to generate a higher turbulence level for inflow B, a custom-made turbulence grid with evenly spaced horizontal and vertical bars is placed at the test section inlet x/D=-2 upstream of the turbine. At the turbine position (x/D=0) a mean streamwise turbulence level of TI_B=10.0% is measured, which decays to 5.5% at x/D=3. Test case B represents turbulence conditions that are comparable to those of a neutral atmospheric boundary layer, although the inevitable decay of the grid-generated turbulence in the experiment is not representative for real conditions. Over the rotor swept area, inflow A is measured to be uniform within $\pm 0.8\%$ in y- and z-direction for all downstream distances. For inflow B, wakes of the single grid bars are still observed at x/D=0, causing a spatial mean velocity variation within $\pm 2.5\%$, while already at x/D=3 the grid-generated turbulent flow is uniform within $\pm 1.0\%$.

The non-uniform shear inflow C is created by a grid with non-uniformly spaced horizontal bars, which is described in more detail in Bartl and Sætran (2017). The vertical flow profile establishes for all streamwise positions and can be approximated by

Table 2. Turbine performance (C_P and C_T) at the optimal operating point ($\lambda = 6.0$) for different yaw angles and inflow conditions.

	Inflow A		Inflow B		Inflow C	
γ [°]	C_P [−]	C_T [−]	C_P [−]	C_T [−]	C_P [−]	C_T [−]
0	0.468	0.893	0.467	0.870	0.459	0.830
+30	0.322	0.707	0.324	0.706	0.321	0.667
-30	0.328	0.711	0.331	0.713	0.327	0.679

the power law

$$\frac{u}{u_{ref}} = \left(\frac{y}{y_{ref}}\right)^{\alpha} \tag{1}$$

in which α describes the strength of the shear profiles gradient du/dy. The grid generated shear flow is approximated by a shear coefficient of $\alpha = 0.11$. Combined with a turbulence intensity of TI_C=10.0%, inflow C resembles conditions measured at an onshore site for a neutral atmospheric boundary layer (Wharton and Lundquist, 2012). In the z-direction, inflow C is measured to be spatially uniform within $\pm 1.0\%$ over the rotor-swept area. The v-component of the flow is observed to be slightly negative for inflow C ranging from v/u_{ref}=[-0.005 -0.080] for all measurement positions. The influence of the negative v-component in the inflow is deemed insignificant for the streamwise velocity u/u_{ref} in the wake. For the analysis of three-dimensional flow effects in the wake the v-component from the inflow is subtracted. All presented mean velocity profiles and turbulence levels are measured in the empty wind tunnel at the reference velocity of $u_{ref} = 10.0 m/s$.

Operating conditions

Figure 3 shows the turbine's measured power and thrust curves for different inflow conditions and yaw angles γ=0° and γ=+30°. In general, power and thrust measurements show very similar behavior for all three inflow conditions as shown in Table 2. Minor differences in the performance curves occur in the transition from stall around λ=3 as previously discussed in Bartl and Sætran (2017).

Performance curves measured for γ=-30° match well with those of γ=+30°, but are not plotted for clarity. For this study, the turbine tip speed ratio is kept constant at its design point at $\lambda_{opt} = 6.0$ for all yaw angles and inflow conditions. For the investigated yaw angles $\gamma = \pm 30°$ the power reduces about 30% compared to the maximum power of the non-yawed turbine. An approximation of this reduction can be obtained with sufficient accuracy by multiplying the maximum power of the non-yawed turbine by $C_{P,A} \cdot cos^3(30°) \approx 0.304$. An adequate estimate of the thrust coefficient of the yawed rotor can be obtained assuming a reduction by $C_{T,A} \cdot cos^2(30°) \approx 0.670$ on the thrust of the non-yawed rotor. This corresponds well to previous measurements by Krogstad and Adaramola (2012).

2.2 Measurement techniques

Power and force measurements

In order to assess the rotor power characteristics, the rotor was installed at another test rig equipped with an HBM torque

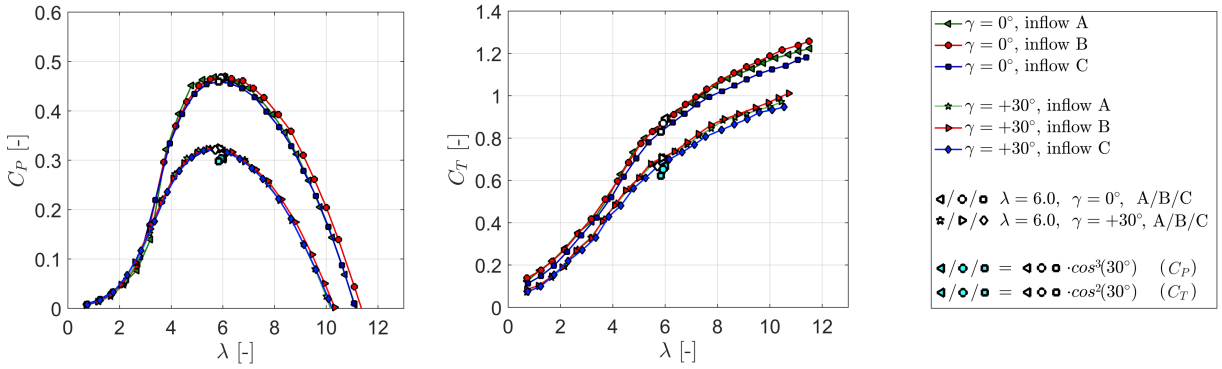

Figure 3. Operating conditions of the model wind turbine: **(a)** power coefficient C_P and **(b)** thrust coefficient C_T for different turbine yaw angels and inflow conditions. The white points indicate the operational conditions, at which wake measurements are performed. Cyan colored points indicate a theoretical power and thrust reduction by yawing of $C_{P,\gamma=0} \cdot cos^3(30°)$ respectively $C_{T,\gamma=0} \cdot cos^2(30°)$.

transducer of the type T20W-N/2-Nm. Flexible couplings connect the torque transducer to the rotor shaft. An optical photo cell is installed on the shaft enabling to measure the rotor rotational speed. The friction in the ball bearing between the rotor and torque sensor is measured without the rotor and thereafter subtracted from the total mechanical power. For the wake measurements the rotor is then installed on a smaller nacelle, which interacts less with the flow. The rotational speed is controlled via a servo motor, ensuring the same power characteristics. For measurements of rotor thrust the model turbine is installed on a six-component force balance produced by Carl Schenck AG.

Flow measurements

The wake flow was measured with a two-component DANTEC FiberFlow Laser Doppler Anemometer (LDA) system used in Differential Doppler Mode. The laser was set up to record the streamwise flow component u as well as the vertical flow component v. In order to obtain results for the lateral flow component w, the laser was turned in $u - w$ direction for one wake measurement. The reference coordinate system and measurement grid is shown in Figure 4. 5×10^4 samples are taken for each measurement point over a period of approximately $30s$, resulting in an average sampling frequency of $1666Hz$. A grid consisting of 357 points is scanned for one full wake contour. For that purpose the LDA system is traversed from -1.0D to +1.0D in z-direction and from -0.8D to +0.8D in y-direction. The distance between two measurement points is $0.1D$. For further analysis, these values are interpolated to a finer grid of $401 \times 321 \approx 129000$ grid points. The natural neighbor interpolation method is used, which gives a smoother interpolation of the value distribution according to Sukumar (1997).

2.3 Measurement uncertainties

The uncertainty of the measured mean velocity is assessed for every sample following the procedure described in Wheeler and Ganji (2004). The LDA manufacturer Dantec Dynamics specifies the uncertainty on measured velocity by 0.04%. Random errors are computed from repeated measurements of various representative measurement points based on a 95 % confidence

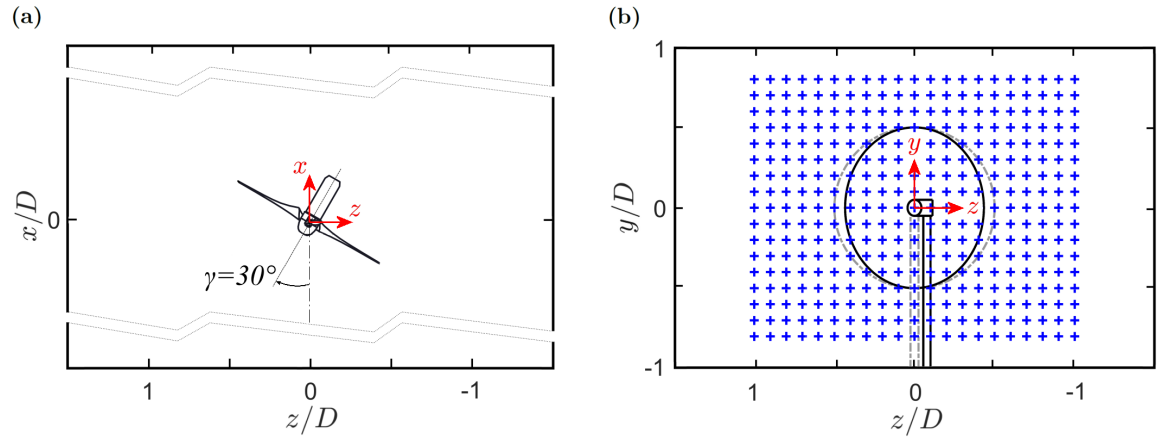

Figure 4. Reference coordinate system in the wind tunnel: **(a)** top view of yawed turbine setup and **(b)** grid for wake measurements.

interval. In the freestream flow as well as in the wake center the calculated uncertainties are below 1%, while increased uncertainties of up to 4% are calculated in the shear layers. Small inaccuracies in the adjustment of the traversing system are deemed to be the main contributor. The uncertainty in turbulent kinetic energy is computed according to the method proposed by Benedict and Gould (1996). Corresponding to the mean velocity the highest uncertainties up to 5% are found in the shear layer between wake and free stream flow.

3 Methods

3.1 Wake shape parametrization

In order to compare the shape of the mean wake for different inflows, the velocity contours are parametrized. The wake contours are therefore sliced into horizontal profiles for each of the 321 interpolated vertical positions. 201 of these 321 velocity profiles are located behind the rotor swept area from y/D=-0.5 to y/D=0.5. These profiles are fitted with an eighth order polynomial to smoothen out local unsteadinesses. Then, an algorithm is applied to locate the z-position of the minimum fitted velocity for each profile. When plotting the z-positions of all these minima versus their y-position, an arc shaped curve is obtained. The curves allow for a direct wake shape comparison depending on inflow condition and yaw angle.

3.2 Wake deflection assessment

As intentional yaw misalignment could possibly be utilized for optimized wind farm control, an exact quantification of the inflow-dependent wake deflection is an important input parameter. However, several methods to quantify the wake deflection have been used in the past, showing a large method-dependent variation in the deflection. Some of these methods are discussed in Section 5. In the present study an available power approach is used, which is deemed to give a solid assessment of the wake deflection. In order to assess the deflection of the wake, the potential power of an imaginary downstream turbine for various

lateral offset positions is calculated. The z-position, at which the available power P^* is minimum, is then defined as the position of wake center deflection $\delta(z/D)$. In this study the available power P^* is calculated for 50 different locations ranging from $-0.5 \leq \mathrm{z/D} \leq 0.5$. The details of the method including an illustration are described in Schottler et al. (2017a).

4 Results

4.1 Mean wake flow

At first the mean wake flows for all three yaw angles $\gamma = [-30, 0, +30]^\circ$, both downstream distances x/D=[3, 6] and all three inflow conditions [A, B, C] are analyzed. Full cross-sectional wake measurements are presented in Figure 5. At the top, the wake flow for inflow A (TI_A=0.23%) is presented. The velocity deficit in the wake is observed to reduce significantly when the turbine is yawed. As the rotor thrust is reduced, a smaller amount of streamwise momentum is lost in x-direction. For a yawed rotor, a cross-stream momentum in z-component is induced. Due to this lateral force component, the wake flow is deflected sideways. This is clearly observed at x/D=3, where the wake is seen to be deflected. Comparing the wake contours at γ=-30° and γ=+30°, an asymmetry in the mean velocity distribution is obvious. The asymmetry between positive and negative wake deflection is even more pronounced at x/D=6, where the wakes are seen to form a kidney shape. Both wake deflection and location of maximum velocity deficit are not symmetric, which is analyzed in more detail in the following sections.

Effects of inflow turbulence

In the center of Figure 5 the mean velocity results of test case B, in which the inflow turbulence level is increased to TI_B=10.0%, are shown. Due to a faster wake recovery the velocity deficits are observed to be smaller for all yaw angles. Increased turbulent mixing smoothened out the gradients between wake and freestream flow compared to test case A. The general wake shape and its lateral deflection for $\gamma = \pm 30^\circ$ is seen to be similar as for the low turbulence inflow. A curled kidney-shaped velocity deficit is also observed at x/D=6 for test case B; however, the curl is not as pronounced as in test case A. Increased mixing might have smoothened the strong gradients in cross-flow direction in this case. The wake behind a positively and negatively yawed turbine appears to feature a higher degree of symmetry than in test case A. Yet an asymmetry of the minimum wake velocity is still obvious for the increased background turbulence level in test case B.

Effects of inflow shear

The wake results for a turbine exposed to inflow shear are shown at the bottom of Figure 5. The turbulence level TI_C=10.0% is the same as in test case B, but shear is present in the inflow. Despite the sheared inflow the wake shapes for all three yaw angles and both downstream distances are observed to be very similar to those of test case B. The normalized velocity levels as well as the inner structure of the wake are almost identical. The influence of shear is however only investigated at high inflow turbulence levels, which does not allow for any conclusions at lower inflow turbulence levels. In the freestream region outside the wake the shear is clearly visible, especially the lower half. Compared to test case B, the wake of the tower is detectable in test case C. The tower wake recovery seems to be slower as the freestream fluid near the tunnel floor contains less kinetic

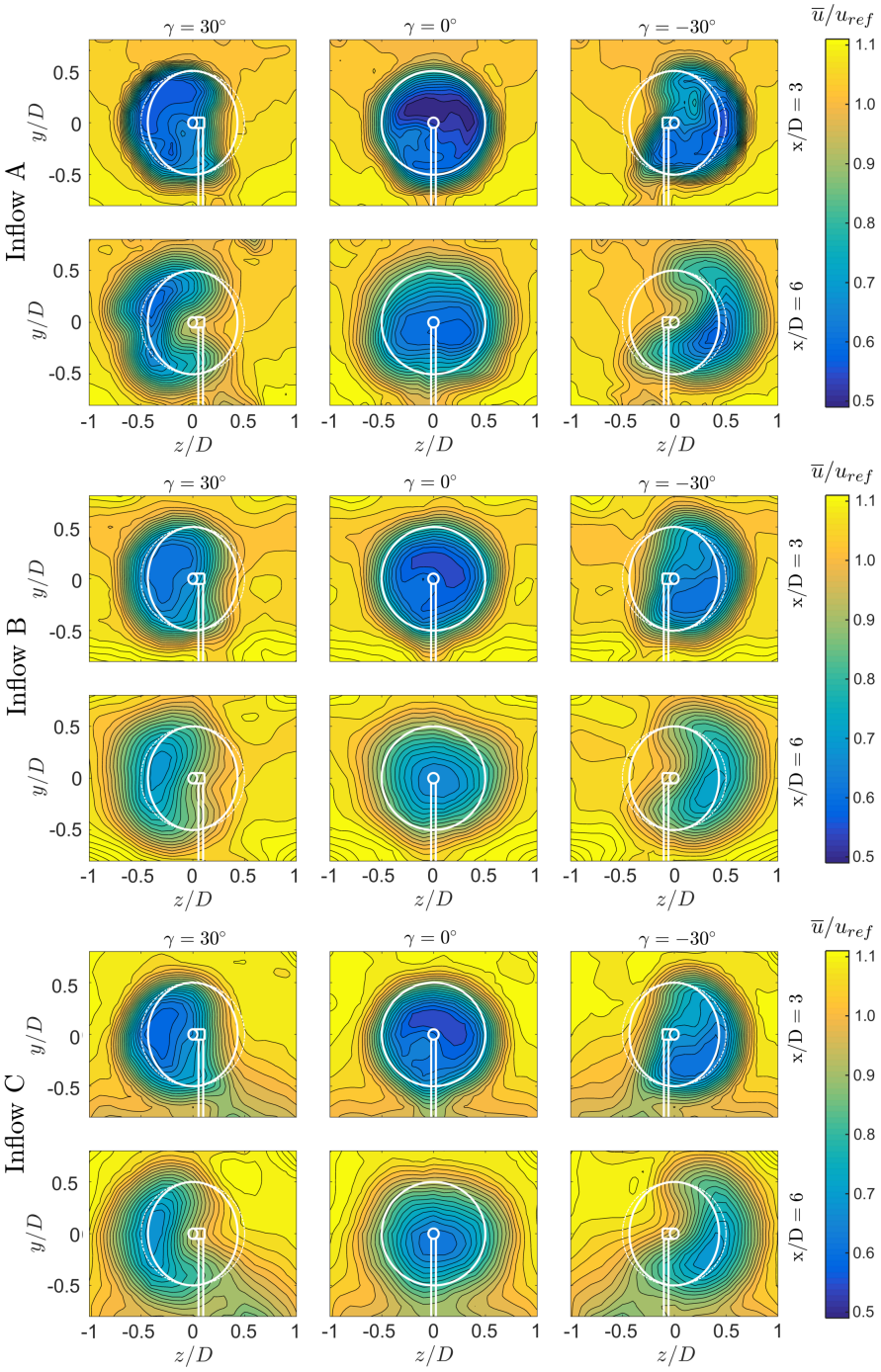

Figure 5. Normalized mean velocity components $\overline{u}/u_{ref}$ for all measured yaw angles $\gamma = [-30, 0, +30]°$, downstream distances x/D=[3, 6] and inflow conditions [A, B, C].

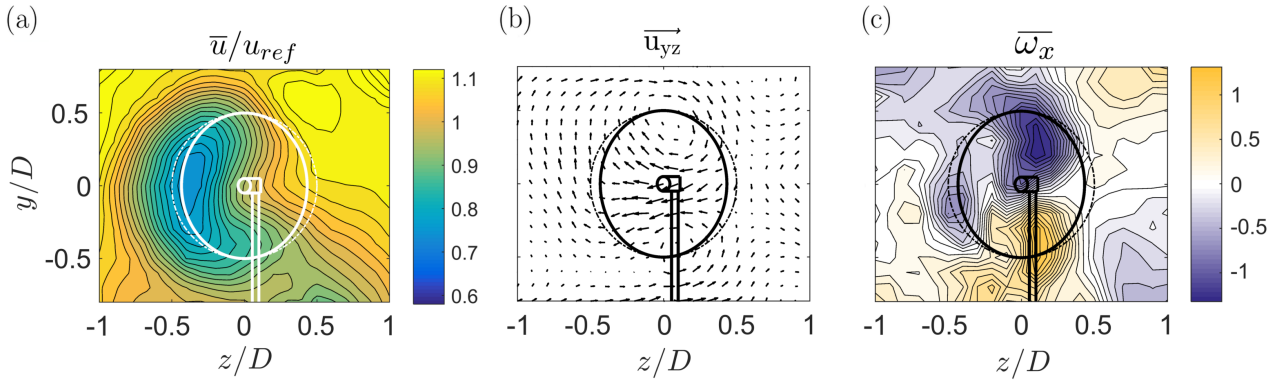

Figure 6. (a) Streamwise mean velocity $\overline{u}/u_{ref}$, **(b)** velocity vector $\boldsymbol{u_{yz}}$ in the yz-plane and **(c)** streamwise mean vorticity $\overline{\omega_x}$ at $\gamma = 30°$ and $x/D = 6$ at inflow C.

energy in test case C.

Curled wake shape

At x/D=6 a kidney-shaped velocity deficit is observed (Figure 5), showing a higher local velocities behind the rotor center. In other words, the maximum wake deflection is found at hub height. The curled kidney shape of the wake can be explained by the formation of a counter-rotating vortex pair, which was previously discussed by Howland et al. (2016) as well as Bastankhah and Porté-Agel (2016). Bastankhah and Porté-Agel also presented a comprehensive explanation by the means of the differential form of the continuity equation. An illustration of the counter-rotating vortex pair at x/D=6 is presented in Figure 6, where the velocity vector $\overrightarrow{u_{yz}}$ as well as the mean streamwise vorticity $\overline{\omega_x}$ are calculated from all three velocity components. The velocity vector in the yz-plane is defined as $\overrightarrow{u_{yz}} = (v, w)$, while the streamwise time-averaged vorticity is defined as $\overline{\omega_x} = \partial v/\partial z - \partial w/\partial y$. As shown in terms of $\overrightarrow{u_{yz}}$ the two vortex centers are formed approximately at the lower and upper boundary of the rotor swept area. The clockwise rotating vortex meets the counter-clockwise rotating vortex in the center behind the wake, leading to strong lateral velocities deflecting the wake sideways.

The locations of high rotation are furthermore visualized by increased levels of vorticity $\overline{\omega_x}$ around the vortex centers. The phenomenon of a counter-rotating vortex pair is not limited to rotating wind turbines. Howland et al. (2016) detected the similar large-scale vortices behind a non-rotating drag disc. Counter-rotating vortex pairs have previously been investigated for jet flows exposed to a cross-flow e.g. by Cortelezzi and Karagozian (2001), a phenomenon which can be interpreted is the inverse to the wake flow behind a skewed rotor. In both phenomena the free shear flow, i.e. a wake or a jet, is superimposed with a strong lateral cross-flow, leading to the formation of a counter-rotating vortex pair at higher downstream distances.

Tower wake deflection

On the bottom of the wake contour plot in Figure 6 (a), the wake of the turbine tower is indicated. The tower wake is observed to be deflected in the opposite direction than the rotor wake when the turbine is yawed. The deflection of the tower wake in

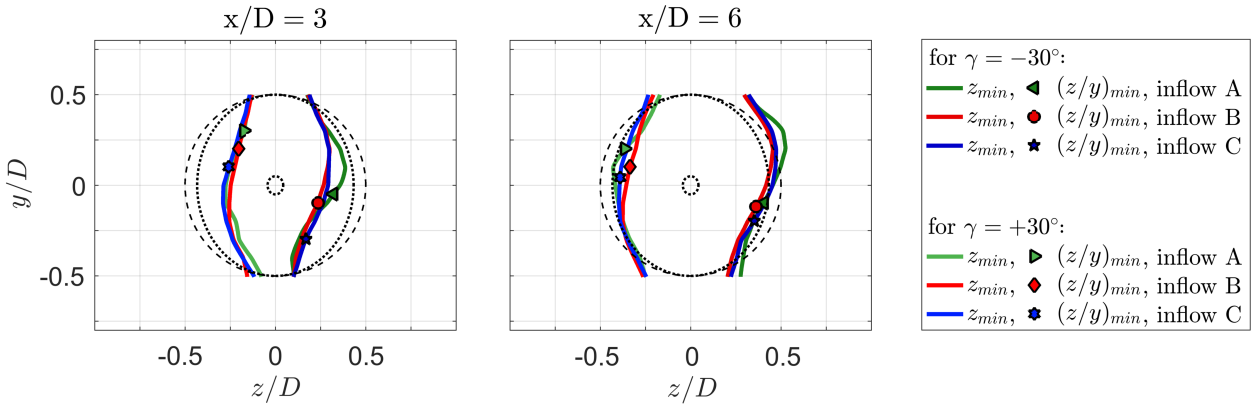

Figure 7. Minimum values in streamwise velocity $\overline{u}/u_{ref}$. Curl shapes and minimum positions are presented at x/D=3 (left) and x/D=6 (right) for the three different inflow conditions.

the opposite direction is believed to have two reasons. Firstly, the turbine tower has a slight offset from z/D=0 as the center of yaw-rotation was set to the rotor midpoint and not the tower. Therefore, a minor offset from the central position is expected for the tower wake. Secondly and more importantly, the tower wake experiences an additional deflection in opposite direction due to an adversely directed cross-flow component outside near the wind tunnel floor as depicted in the vector plot in Figure 6 (b). This cross-flow balances the counter-rotating vortex pair above and possibly deflects the tower wake further to the side.

Wake curl symmetry

In order to compare the three-dimensional wake shapes behind a positively versus negatively yawed turbine more quantitatively, the curled shapes of the velocity deficit area are parametrized to a two-dimensional line. For this purpose, the minimum values in streamwise velocity $\overline{u}/u_{ref}$ are extracted from the fitted wake contours for each vertical position ranging from y/D=[-0.5, ..., 0.5]. The detailed method is described in Section 3.1. This results in the z_{min} lines as presented in Figure 7, which indicate the inflow-dependent wake curl. In addition to that, the position of the minimum velocity $(z/y)_{min}$ in both y- and z-direction is extracted and depicted in the plot by different symbols. The z_{min} lines for all inflow conditions are observed to be slightly tilted in clockwise direction for both downstream distances x/D=3 and x/D=6. The counter-clockwise rotating turbine induces an initial clockwise rotation to the wake flow. Superimposing the clockwise wake rotation with the counter-rotating vortex pair thus results in a slightly tilted curled wake shape. As previously mentioned the wake curl is seen to be more asymmetric for the low background turbulence test case A. A significant bulge is visible for γ=-30° in the upper half of the wake for both downstream positions. For inflow conditions B and C the curl parametrization lines are almost coinciding, confirming the insignificant influence of the moderately sheared inflow on the wake shape. Analyzing the locations of minimum velocities $(z/y)_{min}$ in the wake contours, a deviation from the horizontal centerline y/D=0 for both positive and negative yaw angles is obvious. For γ=-30° the minimum velocities $(z/y)_{min}$ are deflected to the lower half of the wake, while an upward deflection

happens for positive yaw angles γ=+30°. In agreement with Bastankhah and Porté-Agel (2016), the wake rotation is assumed to turn the velocity minimum in clockwise direction initially. The deflection from the wake centerline is observed to be larger for x/D=3 than for x/D=6, where mixing processes already have smoothened the gradients. In the case of sheared inflow of test case C, the locations of minimum wake velocity $(z/y)_{min}$ are found to be lower than for test cases A and B.

Overall wake deflection

The three-dimensional Available power method is used to quantify the overall deflection of the kinetic energy contained in the wake. As explained in Section 3.2 the minimum available power in a circular area in the wake is located, which is reducing the full wake flow field to a single parameter representing the overall wake deflection. A comparison of the minimum available power in the wakes behind a positively versus negatively yawed turbine enables a comparison of symmetry in the deflection of the energy contained in the wake with respect to the yaw angle. Additionally, a two-dimensional Gaussian fit method for the wake center detection at the turbine's hub-height is used to demonstrate systematic differences in the deflection quantification methods. In order to judge possible blockage effects, another rotor of a smaller diameter ($D_{Rot,small}$=0.45 m, $\sigma_{Blockage,small} = \frac{A_{Rot,small}}{A_{Tunnel}}$=3.3%) was used in addition to the 0.90 m ($\sigma_{Blockage,large}$=12.8%) rotor. The details of the experimental setup featuring the smaller 0.45 m rotor are described in Bartl et al. (2018). Further, the results are compared with two different wake models by Jiménez et al. (2010) (JCM) and Bastankhah and Porté-Agel (2016) (BPA). The recommended default model-parameters were used in the implementation of both wake deflection models. For the JCM-model a linear wake expansion factor of $\beta = 0.125$ was applied, while $k_y = 0.022$, $k_z = 0.022$, $\alpha^* = 2.32$ and $\beta^* = 0.154$ were used in the case of the BPA-model. The comparisons of the wake deflections are shown in Figure 8. At x/D=3 the wake deflection for γ=+30° of the smaller rotor and the original rotor match very well. At x/D=6 a small deviation in the wake deflection after the rotors of different sizes and blockage is calculated. It can be assumed that blockage by the wind tunnel walls influences the wake deflection; however, the difference in deflection between the different rotors is observed to be rather small. Comparing the measured deflection with the prediction models discloses larger deviations. The deflection predicted by the JCM-model is generally observed to be larger than the one predicted by the BPA-model. The calculated wake deflection by the available power method at x/D=3 is still well predicted by the BPA-model, while more significant deviations are observed at x/D=6. Obviously larger differences in wake deflection are predicted by the JCM-model, both at x/D=3 and x/D=6. A number of reasons are possible to cause the significant deviations between measured and modeled deflection results. Besides the discussed wind tunnel blockage, a major source of uncertainty in this comparison arises from the method used to calculate the wake deflection. Quantifying the wake deflection by he minimum of a fitted Gaussian on the hub height velocity profiles results in a better match with the BPA-model at x/D=6 as shown by the red curve in Figure 8. However, using the hub height profile only for the wake center deflection does not take the total mean kinetic energy content in the wake into account. Due to the complex three dimensional shape of the velocity deficit, a reduction of the wake deflection to one single value has been shown to be difficult A number of different methods have been proposed, resulting in many different deflection quantifications (Vollmer et al., 2016). Further, the wake deflection $\delta(z/D)$ for all three inflow conditions is compared. These results are shown in Figure 9 and compared to the BPA-model. In contrast to the JCM-model, the inflow turbulence intensity is an input variable in the BPA-model. It

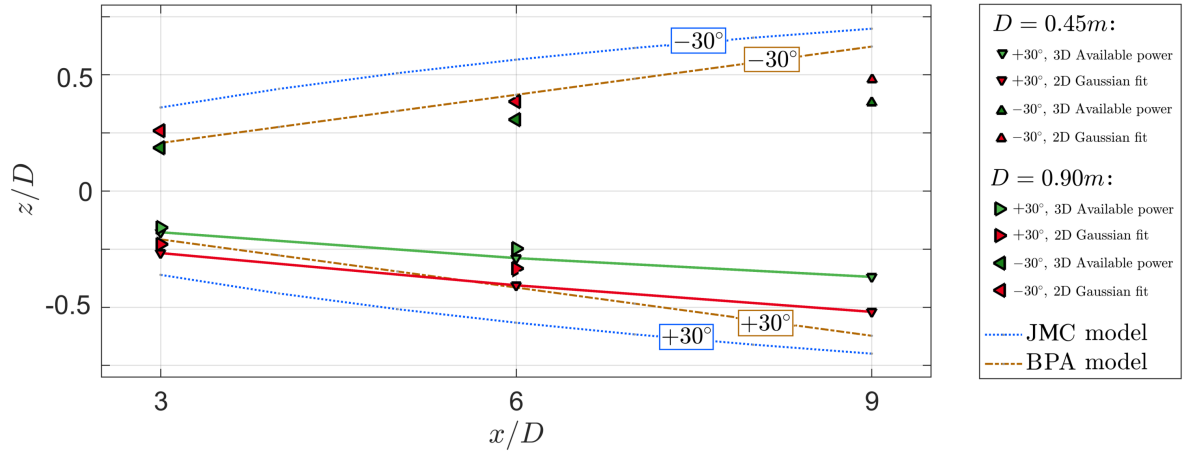

Figure 8. Calculated wake deflection $\delta(z/D)$ for the NTNU rotor ($D = 0.90m$), a downscaled NTNU rotor ($D = 0.45m$) as well as Jiménez et al.'s and Bastankhah and Porte-Agél's wake deflection model. The inflow turbulence level is $TI_A = 0.23\%$.

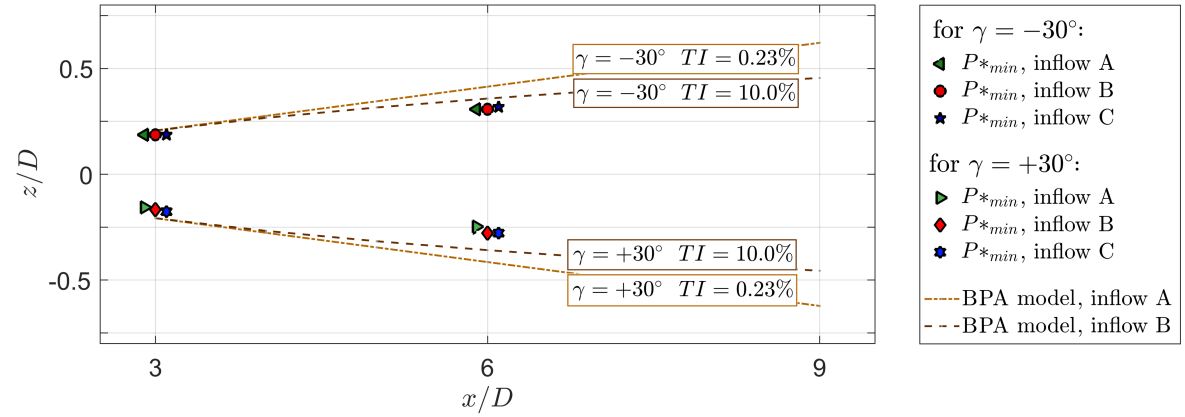

Figure 9. Calculated wake deflection $\delta(z/D)$ at x/D=3 and x/D=6 for three different inflow conditions A, B and C compared to TI-dependent deflection predictions by Bastankhah and Porte-Agél's wake deflection model. Note that a small offset in x/D of the measured values was chosen for better visibility.

can be observed that the BPA-model predicts a higher wake deflection for a smaller inflow turbulence level. Bastankhah and Porté-Agel (2016) argue that smaller inflow turbulence reduces the flow entrainment in the far wake and thus increases the wake deflection. The calculated lateral deflection values $\delta(z/D)$ and the associated wake skew angle ξ are furthermore listed in Table 3.

In general, a very similar wake deflection is observed for all three inflow conditions at both downstream distances. A systematic asymmetry in the wake deflection represented by the minimum available power behind a turbine yawed γ=-30° and

Table 3. Lateral deflection $\delta(z/D)$ [−] and wake skew angle ξ [°] calculated with the available power method.

		Inflow A		Inflow B		Inflow C	
γ [°]	x/D [−]	$\delta(z/D)$	ξ [°]	$\delta(z/D)$	ξ [°]	$\delta(z/D)$	ξ [°]
0	3	0.015	0.29	0.005	0.10	0.015	0.29
+30	3	-0.157	-2.99	-0.167	-3.18	-0.177	-3.38
-30	3	0.187	3.57	0.187	3.57	0.187	3.57
0	6	0.026	0.24	0.036	0.34	0.036	0.34
+30	6	-0.248	-2.36	-0.278	-2.65	-0.278	-2.65
-30	6	0.308	2.94	0.308	2.94	0.318	3.03

γ=+30° is observed. The wake shows a higher deflection for negative yaw angles in all inflow cases. Also the wake behind the non-yawed turbine is seen to be slightly deflected in positive z-direction, which is assumed to stem from the interaction of the rotating wake with the turbine tower. As discussed by Pierella and Sætran (2017) who performed experiments on the same rotor with a larger tower, the tower-wake-interaction leads to an uneven momentum entrainment in the wake. For a non-yawed setup, they observed both a lateral and vertical displacement of the wake vortex center, induced by an interaction with the tower wake. It can therefore be assumed that also the interaction of the counter-rotating vortex pair with the tower wake slightly displaced wake vortex in the yawed cases might be influence by an interaction with the tower wake, which is the only source of asymmetry in an otherwise perfectly symmetrical setup. Increasing the turbulence level from TI_A=0.23% to TI_B=10.00% is found to only have a small influence on the wake deflection. In fact, no difference is detected for γ=-30°. For γ=+30°, however, a slightly smaller wake deflection is calculated for the lower inflow turbulence. This can also be interpreted as a higher degree of asymmetry for low background turbulence. Adding shear to the inflow is not observed to change the wake deflection significantly. This confirms the above-mentioned similarity in wake shapes measured for test cases B and C.

4.2 Rotor-generated turbulence

For the measurements presented in the this study the kinetic energy is considered to be fully dominated by turbulent motions from $x/D \geq$3 for inflow A, as Eriksen and Krogstad (2017) recently showed that the production of rotor-generated turbulent kinetic energy is finished at x/D=3 for measurements on the same rotor and inflow condition. For inflow conditions B and C, the transition to fully turbulent motions is expected to take place at even smaller downstream distances.

Effects of yawing on turbulent kinetic energy distributions

At the top of Figure 10 the TKE levels in the wake are presented for test case A (TI_A=0.23%). As observed in earlier studies (Bartl and Sætran, 2017; Eriksen and Krogstad, 2017) a ring of high turbulence levels is formed behind the tips of the rotor blades for a non-yawed turbine. In this region the tip vortices decayed into turbulent motions. With increasing downstream distance the sharp peaks decrease in magnitude and blur out to their surrounding. For a yawed turbine, the ring of peak turbulence

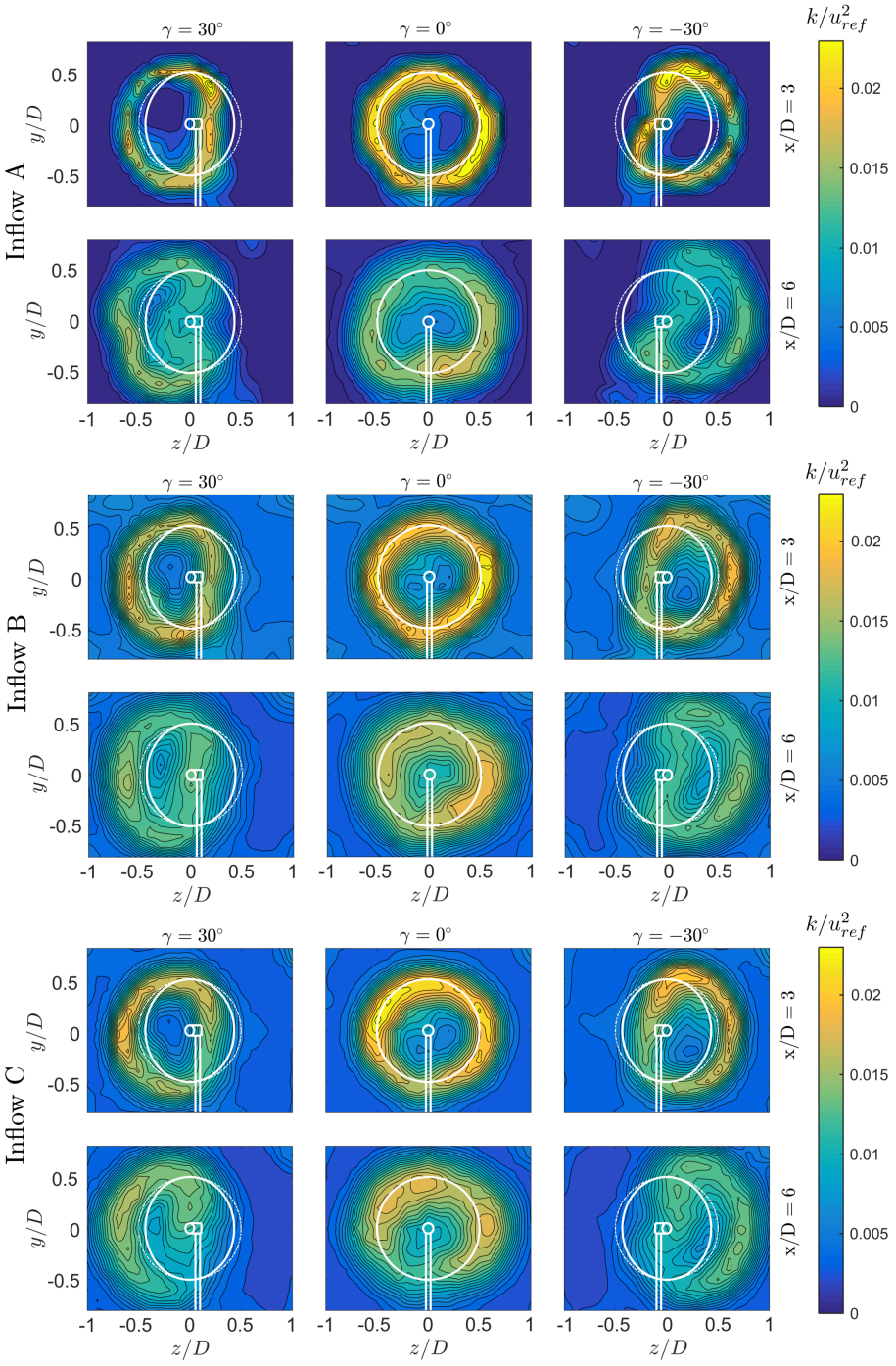

Figure 10. Turbulent kinetic energy k/u_{ref}^2 for all measured yaw angles $\gamma = [-30, 0, +30]°$, downstream distances x/D=[3, 6] and inflow conditions [A, B, C].

is laterally deflected and deformed accordingly. For x/D=3 the peaks are clearly separated by an area of low turbulence in the center of the deflected wake. For x/D=6, this area is observed to be significantly smaller. The peaks are still distinct, but it is expected that they start merging into one peak for higher downstream distances. The strongest TKE levels are observed for locations of the highest gradient in mean streamwise velocity. Thus, the TKE-ring's extension is observed to be slightly larger than the contours of the mean streamwise velocity, emphasizing the need to take the parameter TKE into account in wind farm site planning or yaw control studies.

Effects of inflow turbulence and shear

The TKE contours for increased inflow turbulence of test case B are shown in the center of Figure 10 as well as the red lines in Figure 11. At x/D=3, slightly smaller TKE peaks and higher centerline turbulence are measured for test case B than for test case A. The higher TKE levels in the freestream lead to an increased mixing, which is reducing the TKE peaks in the tip region. At x/D=6 the TKE peaks are observed to be at about the same level for both inflow conditions. For the yawed cases also the turbulence level in the wake center has evened out between inflow cases A and B. The TKE levels for the sheared inflow in test case C are observed to be very similar to those of test case B for all investigated yaw angles. These findings suggest that the presence of a moderate shear flow in a highly turbulent boundary layer does not influence the production of rotor-generated turbulent kinetic energy significantly.

Approximation for turbulent kinetic energy distributions in yaw

The levels of peak turbulence are observed to decrease considerably when the rotor is yawed. For a direct case-to-case comparison, TKE-profiles at hub height y=0 at x/D=6 are presented for $\gamma = 0°$ and $\gamma = -30°$ in the lower plots of Figure 11. For a yawed turbine, the rotor thrust reduces with approximately $cos^2(\gamma)$ as previously shown in Figure 3. Multiplying also the TKE levels generated by the non-yawed rotor with $cos^2(\gamma)$ is observed to result in a decent first order approximation of the turbulence levels behind the yawed rotor. The reduced TKE levels for $\gamma = -30°$ are indicated by the chain-dotted lines in the lower left plot of Figure 11. For an approximation of the lateral deflection of the turbulence peaks for yawed rotors, their location can be estimated as proposed by Schottler et al. (2018). In this approach the expected value and standard deviation of a Gaussian fit of the velocity profile behind a yawed rotor is calculated. Adding the standard deviation to the expected value $\mu \pm \sigma_u$ gives a rough estimate of the locations of the corresponding TKE peaks, as shown by the vertical lines in Figure 11. Thus, it is possible to approximate both TKE peak locations and levels by knowing TKE and mean velocity for the now-yawed case. This might be a useful addition for modeling the rotor-generated turbulence in yawed wakes. For a complete assessment of mean velocity and turbulent kinetic energy in a yawed wind turbine wake, the model for streamwise velocity profiles by Bastankhah and Porté-Agel (2016) could be extended by the proposed relations for the rotor generated turbulence.

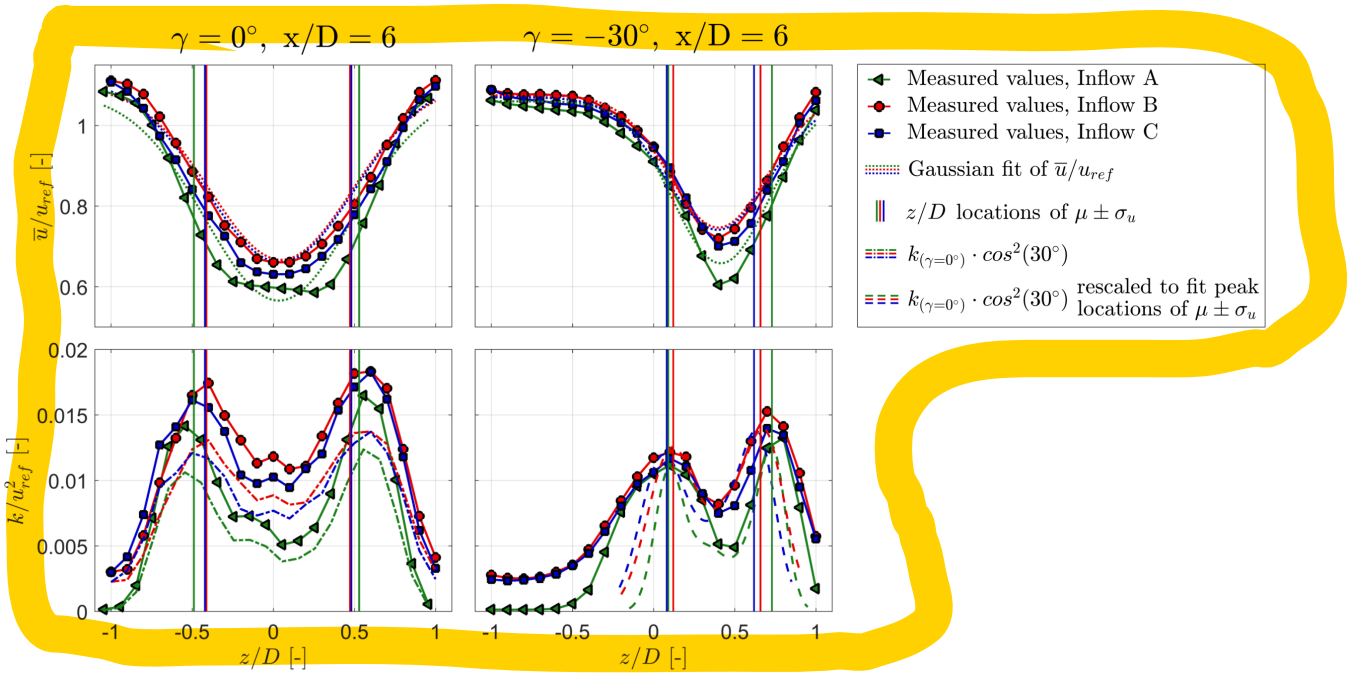

Figure 11. Normalized mean velocity and turbulent kinetic energy k/u_{ref}^2 profiles at hub height $y = 0$ and x/D=6. The yaw angles are set to $\gamma = 0°$ and $\gamma = -30°$. Vertical lines indicate the borders of standard deviations of Gaussian-fitted velocity profiles $\mu \pm \sigma_u$. Chain-dotted lines indicate a TKE profiles at $\gamma = 0°$ multiplied by $cos^2(-30°)$. Dashed lines in the lower right subplot have the same magnitude as the chain-dotted lines, but are linearly scaled in z to fit the peak locations of $\mu \pm \sigma_u$.

5 Discussion

The present wind tunnel investigation showed detailed flow measurements in the wake of a yawed model turbine for different inflow conditions. A number of modeling techniques and turbine sizes were used in previous yaw wake studies in the literature, resulting in a significant variation in wake shapes and their deflection. However, a number of general flow effects in the wake behind a yawed turbine seem to be reproducible

Our results indicated minor asymmetries in the wake flow behind positively and negatively yawed turbines. The interference of the modified flow field around the tower and wake rotation is deemed to be the source for this asymmetry. This explanation is consistent with findings by Grant and Parkin (2000), who reported clear asymmetries in the tip vortex shedding and circulation in the wake for positive and negative yaw angles. Our experimental measurements showed a kidney shaped mean velocity deficit at x/D=6 for all inflow conditions. These results agree well with recently discussed experimental results by Howland et al. (2016). Although the wake shape was not specifically discussed, a curled wake shape was already indicated in the results presented by Medici and Alfredsson (2006). The results presented by Bastankhah and Porté-Agel (2016) offer a good comparison as wakes were measured at a number of yaw angles and downstream distances. The wake shape and velocity deficit at $\gamma = \pm 30°$ and x/D=6 match qualitatively well with our results, when an opposite sense of turbine rotation is taken

into account. A direct comparison of the wakes at x/D=3 and x/D=6 of the here presented results of test case B with an equivalent setup for a slightly smaller model turbine of different rotor geometry was performed by Schottler et al. (2017b) and Schottler et al. (2018). These results show a more distinct curl in the wake already at x/D=3 while velocity deficit and wake deflection are generally found to be very similar for both model turbines.

Our study moreover indicates that the wake shape and deflection is affected by inflow turbulence. The overall wake deflection was observed to be similar for both investigated turbulence levels. For a more detailed investigation of diffusion mechanisms in the wake, however, a vorticity analysis in the wake of a turbine exposed to low and high turbulence is motivated for future studies. The inflow turbulence is furthermore implemented as an input parameter in the recently developed wake model by Bastankhah and Porté-Agel (2016). The influence of the inflow turbulence seems to be slightly overpredicted by their model, although a more thorough analysis for different yaw angles and downstream distances on a smaller, unblocked rotor are needed for a solid assessment of the model's sensitivity to inflow turbulence. Furthermore, the comparison of the model-predicted deflection and experimentally obtained results is not straightforward. Due to the various different calculation methods used the assessment of the wake center deflection is found to be equivocal. Gaussian fitting to locate the minimum wake velocity was amongst others used by Jiménez et al. (2010) as well as Fleming et al. (2014), while Luo et al. (2015) and Howland et al. (2016) calculated the center of mass of the three-dimensional velocity contour. A comparison of different wake deflection methods was presented by Vollmer et al. (2016), showing the significant method-related variation in deflection quantification.

Another focus of the present study was to assess whether the wake's properties are significantly influenced by sheared inflow. Shear is present in most atmospheric boundary layer flows and highly dependent on stability and the terrain's complexity and roughness. The strength of the investigated shear in test case C is rather moderate and considered typical for a neutral atmospheric boundary layer (Wharton and Lundquist, 2012). As the study investigated only two different shear flows (α_B=0.0 and α_C=0.11), solid statements about the wake flow's sensitivity to this parameter cannot be made. The results do however indicate a rather insignificant effect of such a moderate shear on the wake flow. Possibly, a considerably stronger shear at lower inflow turbulence would have resulted in more distinguishable wake characteristics. In contrast to a recent full-scale LES study by Vollmer et al. (2016), our results seem to shown a rather small dependency of the wake characteristics on the inflow conditions. However, Vollmer et al. (2016) varied four different inflow parameters (turbulence intensity, potential temperature wind shear and veer) simultaneously, which made direct conclusions on the sensitivity to a single inflow parameter difficult. In conclusion, our results do not contradict with their findings as the inflow conditions in both setups were modeled very differently.

6 Conclusions

An experimental study on the inflow-dependent wake characteristics of a yawed model wind turbine was realized. In accordance with previous studies, it is confirmed that intentional turbine yaw misalignment is an effective method to laterally deflect the velocity deficit in the wake and thus offers a large potential for power optimization in wind farms. For the equally important optimization of downstream turbine fatigue loads, a careful planning of wind farm layout and control strategy should thus

also take the strength and expansion of rotor-generated turbulence footprints into account. We show that the rotor-generated turbulence distributions are deflected in the same degree as the mean velocity profiles, but feature a slightly wider expansion. Further analysis demonstrated that an increasing yaw angle reduces the levels of the peak turbulence, which is decreasing at a similar rate as the rotor thrust.

The study moreover recommends a consideration of the inflow turbulence level as an important parameter for deflection models implemented in wind farm controllers, as it is affecting the yaw-angle dependent symmetry in shape and deflection. The degree of asymmetry was observed to be higher for lower inflow turbulence. The recently proposed wake deflection model by Bastankhah and Porté-Agel (2016) proved to deliver good approximations of inflow-turbulence-dependent wake deflection. However, more wake measurements at different yaw angles and various downstream distances should be performed to fully assess the model's sensitivity to inflow turbulence. As the influence of a gentle inflow-shear on the wake characteristics was found to be insignificant, an inclusion of this parameter in wake models is thus not considered to be essential at this stage. The experimental results revealed very similar velocity deficit and rotor-generated turbulence distributions to those measured for an uniform inflow.

Data availability. All presented wake data in this paper is available on *https://doi.org/10.5281/zenodo.1193656*

Competing interests. The authors declare that there are no competing interests.

Acknowledgements. The authors would like to acknowledge the IPID4all travel support granted by the German Academic Exchange Service (DAAD).

References

Annoni, J., Gebraad, P., Scholbrock, A., Fleming, P., and van Wingerden, J.-W.: Analysis of axial-induction-based wind plant control using an engineering and a high-order wind plant model, Wind Energy, 19, 113–1150, doi:10.1002/we.1891, 2016.

Barthelmie, R. J., Pryor, S. C., Frandsen, S. T., Hansen, K. S., Schepers, J. G., Rados, K., Schlez, W., Neubert, a., Jensen, L. E., and Neckelmann, S.: Quantifying the impact of wind turbine wakes on power output at offshore wind farms, Journal of Atmospheric and Oceanic Technology, 27, 1302–1317, doi:10.1175/2010JTECHA1398.1, 2010.

Bartl, J. and Sætran, L.: Experimental testing of axial induction based control strategies for wake control and wind farm optimization, Journal of Physics: Conference Series, 753, 032 035, doi:10.1088/1742-6596/753/3/032035, 2016.

Bartl, J. and Sætran, L.: Blind test comparison of the performance and wake flow between two in-line wind turbines exposed to different turbulent inflow conditions, Wind Energy Science, 2, 55–76, doi:10.5194/wes-2-55-2017, 2017.

Bartl, J., Müller, A., Landolt, A., Mühle, F., Vatn, M., Oggiano, L., and Sætran, L.: Validation of the real-time-response ProCap measurement system for full wake scans behind a yawed model-scale wind turbine, Manuscript submitted to Journal of Physics: Conference Series, DeepWind 2018 Conference, 2018.

Bastankhah, M. and Porté-Agel, F.: Experimental and theoretical study of wind turbine wakes in yawed conditions, Journal of Fluid Mechanics, 806, 506–541, doi:10.1017/jfm.2016.595, 2016.

Benedict, L. and Gould, R.: Towards better uncertainty estimates for turbulence statistics, Experiments in Fluids, 22, 129–136, doi:10.1007/s003480050030, 1996.

Berdowski, T., Ferreira, C., van Zuijlen, A., and van Bussel, G.: Three-Dimensional Free-Wake Vortex Simulations of an Actuator Disc in Yaw, AIAA SciTech Forum, Wind Energy Synopsium 2018, doi:10.2514/6.2018-0513, 2018.

Cortelezzi, L. and Karagozian, A.: On the formation of the counter-rotating vortex pair in transverse jets, Journal of Fluid Mechanics, 446, 347–373, doi:10.1017/S0022112001005894, 2001.

Eriksen, P. E. and Krogstad, P.-Å.: Development of coherent motion in the wake of a model wind turbine, Renewable Energy, 108, 449–460, doi:10.1016/j.renene.2017.02.031, 2017.

Fleming, P., Gebraad, P., Lee, S., van Wingerden, J.-W., Johnson, K., Churchfield, M., Michalakes, J., Spalart, P., and Moriarty, P.: Evaluating techniques for redirecting turbine wakes using SOWFA, Renewable Energy, 70, 211–218, doi:10.1016/j.renene.2014.02.015, 2014.

Fleming, P., Gebraad, P., Lee, S., van Wingerden, J.-W., Johnson, K., Churchfield, M., Michalakes, J., Spalart, P., and Moriarty, P.: Simulation comparison of wake mitigation control strategies for a two-turbine case, Wind Energy, 18, 2135–2143, doi:10.1002/we.1810, 2015.

Fleming, P., Annoni, J., Churchfield, M., Martinez, L., Gruchalla, K., Lawson, M., and Moriarty, P.: From wake steering to flow control, Wind Energ. Sci. Disc., doi:10.5194/wes-2017-52, 2017.

Gebraad, P. M. O., Fleming, P. A., and van Wingerden, J. W.: Comparison of Actuation Methods for Wake Control in Wind Plants, American Control Conference, doi:10.1109/ACC.2015.7170977, 2015.

Gebraad, P. M. O., Teeuwisse, F. W., van Wingerden, J. W., Fleming, P. A., Ruben, S. D., Marden, J. R., and Pao, L. Y.: Wind plant power optimization through yaw control using a parametric model for wake effects-a CFD simulation study, Wind Energy, 19, 95–114, doi:10.1002/we.1822, 2016.

Grant, I. and Parkin, P.: A DPIV study of the trailing vortex elements from the blades of a horizontal axis wind turbine in yaw, Experiments in Fluids, 28, 368–376, doi:10.1007/s003480050, 2000.

Grant, I., Parkin, P., and Wang, X.: Optical vortex tracking studies of a horizontal axis wind turbine in yaw using laser-sheet, flow visualisation, Experiments in Fluids, 23, 513–519, doi:10.1007/s003480050, 1997.

Haans, W., Sant, T., van Kuik, G., and van Bussel, G.: Measurement of Tip Vortex Paths in the Wake of a HAWT Under Yawed Flow Conditions, Journal of Solar Energy Engineering, 127, 456–463, doi:10.1115/1.2037092, 2005.

Howland, M. F., Bossuyt, J., and Mart, L. A.: Wake Structure of Wind Turbines in Yaw under Uniform Inflow Conditions, Journal of Renewable and Sustainable Energy, 8, 043 301, doi:10.1063/1.4955091, 2016.

Jiménez, Á., Crespo, A., and Migoya, E.: Application of a LES technique to characterize the wake deflection of a wind turbine in yaw, Wind Energy, 13, 559–572, doi:10.1002/we.380, 2010.

Knudsen, T., Bak, T., and Svenstrup, M.: Survey of wind farm control—power and fatigue optimization, Wind Energy, 18, 1333–1351, doi:10.1002/we.1760, 2014.

Krogstad, P.-Å. and Adaramola, M. S.: Performance and near wake measurements of a model horizontal axis wind turbine, Wind Energy, 15, 743–756, doi:10.1002/we.502, 2012.

Luo, L., Srivastava, N., and Ramaprabhu, P.: A Study of Intensified Wake Deflection by Multiple Yawed Turbines based on Large Eddy Simulations, AIAA SciTech Forum, (AIAA 2015-0220), doi:10.2514/6.2015-0220, 2015.

Medici, D. and Alfredsson, P. H.: Measurements on a wind turbine wake: 3D effects and bluff body vortex shedding, Wind Energy, 9, 219–236, doi:10.1002/we.156, 2006.

Pierella, F. and Sætran, L.: Wind tunnel investigation on the effect of the turbine tower on wind turbines wake symmetry, Wind Energy, doi:10.1002/we.2120, 2017.

Schepers, J. G.: An Engineering Model For Yawed Conditions, Developed On Basis Of Wind Tunnel Measurements, American Institute of Aeronautics and Astronautics, 99-0039, 164–174, doi:10.2514/6.1999-39, 1999.

Schepers, J. G., K. Boorsma, K., and Munduate, X.: Final Results from Mexnext-I: Analysis of detailed aerodynamic measurements on a 4.5 m diameter rotor placed in the large German Dutch Wind Tunnel DNW, Journal of Physics: Conference Series, 555, 012 089, doi:10.1088/1742-6596/555/1/012089, 2014.

Schottler, J., Hölling, A., Peinke, J., and Hölling, M.: Wind tunnel tests on controllable model wind turbines in yaw, AIAA 34th Wind Energy Symposium, p. 1523, doi:10.2514/6.2016-1523, 2016.

Schottler, J., Hölling, A., Peinke, J., and Hölling, M.: Brief communication: On the influence of vertical wind shear on the combined power output of two model wind turbines in yaw, Wind Energy Science, 2, 439–442, doi:10.5194/wes-2-439-2017, 2017a.

Schottler, J., Mühle, F., Bartl, J., Peinke, J., Adaramola, M. S., Sætran, L., and Hölling, M.: Comparative study on the wake deflection behind yawed wind turbine models, Journal of Physics: Conference Series, 854, 012 032, doi:10.1088/1742-6596/854/1/012032, 2017b.

Schottler, J., Bartl, J., Mühle, F., Sætran, L., Peinke, J., and Hölling, M.: Wind tunnel experiments on wind turbine wakes in yaw: Redefining the wake width, In review in Wind Energ. Sci. Discuss., 2018.

Sukumar, N.: A Note on Natural Neighbor Interpolation and the Natural Element Method (NEM), Theoretical and Applied Mechanics, Northwestern University, IL 60208, (last access: 25 February 2017), 1997.

Thomsen, K. and Sørensen, P.: Fatigue loads for wind turbines operating in wakes, Journal of Wind Engineering and Industrial Aerodynamics, 80, 121–136, doi:10.1016/S0167-6105(98)00194-9, 1999.

Vollmer, L., Steinfeld, G., Heinemann, D., and Kühn, M.: Estimating the wake deflection downstream of a wind turbine in different atmospheric stabilities: an LES study, Wind Energy Science, 1, 129–141, doi:10.5194/wes-1-129-2016, 2016.

Wang, J., Foley, S., Nanos, E. M., Yu, T., Campagnolo, F., Bottasso, C. L., Zanotti, A., and Croce, A.: Numerical and Experimental Study of Wake Redirection Techniques in a Boundary Layer Wind Tunnel, Journal of Physics: Conference Series, 854, 012 048, doi:10.1088/1742-6596/854/1/012048, 2017.

Wharton, S. and Lundquist, J. K.: Assessing atmospheric stability and its impacts on rotor-disk wind characteristics at an onshore wind farm, Wind Energy, 15, 525–546, doi:10.1002/we.483, 2012.

Wheeler, A. J. and Ganji, A. R.: Introduction to engineering experimentation, Upper Saddle River, NJ, USA, Pearson/Prentice Hall, XI, third edition edn., 2004.